

Estimates on the possible annual seismicity of Venus

Iris van Zelst^{1,2}, Julia Maia^{1,3}, Ana-Catalina Plesa¹, Richard Ghail⁴, Moritz Spühler¹

¹Institute of Planetary Research, German Aerospace Center (DLR), Berlin, Germany

²Centre of Astronomy and Astrophysics, Technical University of Berlin, Berlin, Germany

³Université Côte d'Azur, Observatoire de la Côte d'Azur, CNRS, Laboratoire Lagrange, Nice, France

⁴Department of Earth Sciences, Royal Holloway, University of London, Egham, UK

Key Points:

- An inactive Venus with global background seismicity like Earth's continental intraplate seismicity has a few hundred quakes $\geq M_w 4$ per year
- A lower bound on an active Venus where fold belts, coronae, and rifts are seismically active predicts a few thousand quakes $\geq M_w 4$ annually
- The upper bound for an active Venus results in thousands ($\sim 5,000 - 18,000$) venusquakes $\geq M_w 4$ per year

This manuscript is a preprint which has been submitted for publication.

It has not undergone peer review yet.

Subsequent versions of this manuscript may have slightly different content.

If accepted, the final version of this manuscript will be available via the 'Peer-reviewed Publication DOI' link on the right-hand side of this webpage. Please feel free to contact any of the authors; we welcome feedback!

15 Abstract

16 There is a growing consensus that Venus is seismically active, although its level of seismicity could be very different from that of Earth due to the lack of plate tectonics. Here, we estimate upper and lower bounds on the expected annual seismicity of Venus by scaling the seismicity of the Earth. We consider different scaling factors for different tectonic settings and account for the lower seismogenic zone thickness of Venus. We find that 95 – 296 venusquakes equal to or bigger than moment magnitude (M_w) 4 per year are expected for an inactive Venus, where the global seismicity rate is assumed to be similar to that of continental intraplate seismicity on Earth. For the active Venus scenarios, we assume that the coronae, fold belts, and rifts of Venus are currently seismically active. This results in 1,161 – 3,609 venusquakes $\geq M_w4$ annually as a realistic lower bound and 5,715 – 17,773 venusquakes $\geq M_w4$ per year as a maximum upper bound for an active Venus.

28 Plain Language Summary

29 Venus could be seismically active at the moment, but it is uncertain how many earthquakes (or to use the proper term: venusquakes) there could be in a year. Here, we calculate the minimum and maximum number of venusquakes we could expect in a given year on Venus based on different assumptions. If we assume there is not much seismic activity on Venus (comparable to the interior of tectonic plates on Earth), we find that we could expect about a few hundred venusquakes per year with a magnitude bigger than or equal to 4. For an estimate of the maximum amount of venusquakes, we assume that Venus has regions with more seismic activity: the so-called coronae, fold belts, and rifts. Depending on our assumptions, we then find that more than 17,000 venusquakes could occur in a year with a magnitude bigger than or equal to 4.

39 1 Introduction

40 After the successful mapping of the Venusian surface by Magellan from 1990 to 1992, for a long time the prevailing hypotheses for Venus’s geodynamic regime were that of a catastrophic or episodic resurfacing regime. The reason for this was the observation of a relatively low number of craters with a near-random spatial distribution on the surface (932 craters; Strom et al., 1994), from which people deduced a uniform, relatively young surface age of 800–240 Myr (McKinnon et al., 1997; Le Feuvre & Wiczorek, 2011). In these catastrophic or episodic resurfacing scenarios, Venus is currently in a relatively quiet tectonic phase after the geologically-recent resurfacing event that led to the observed young surface age (Rolf et al., 2022; O’Rourke et al., 2023). However, the impact crater observations are also consistent with models in which volcanic and tectonic activity occurs at roughly constant rates over time (e.g., Herrick et al., 2023).

51 Indeed, in recent years the view on Venus’s current tectonic activity has shifted towards a more active planet, rivalled in the Solar System only, perhaps, by our own Earth. From a geodynamical point of view, other theories for its geodynamic regime have been put forward, such as the plutonic squishy lid regime (Lourenço et al., 2020), which are consistent with ongoing activity on Venus today. Additionally, the shift towards an active Venus is partly induced by compelling evidence from Magellan, Pioneer Venus, and Venus Express data that Venus might be currently volcanically active. Data from Venus Express shows regions of high emissivity which could be associated with chemically unweathered rocks (Smrekar et al., 2010). The emissivity anomalies correlate with volcanic rises, such as Imdr Regio (Smrekar et al., 2010), indicating geologically recent volcanism in these regions. Depending on the assumption of tectonic regime and amount of volcanic flux, Smrekar et al. (2010) estimate that the bright spots represent recently active volcanoes younger than ~ 2.5 Myr, and potentially much younger (250,000 years old

64 or less). Various weathering experiments at Venusian temperatures (see M. S. Gilmore
 65 et al., 2023, for an overview) have even suggested that the reduction of surface emis-
 66 sivity is a rapid process on the order of tens to hundreds of years (Zhong et al., 2023)
 67 or even months to years (Filiberto et al., 2020). Brossier et al. (2022) therefore postu-
 68 late that the low radar emissivity values in Ganis chasma could be the result of volcanic
 69 eruptions in the last 30 years, indicating that Venus is volcanically active now (Filiberto
 70 et al., 2020). The variability in SO_2 concentration in the clouds observed by Pioneer Venus
 71 and Venus Express from 1979 to 2011 could also be attributed to recent volcanic erup-
 72 tions (Marcq et al., 2013). The most compelling evidence for active volcanism on Venus
 73 to date comes from Herrick and Hensley (2023), who observed changes in a volcanic re-
 74 gion by analysing consecutive radar images acquired by Magellan. They interpreted these
 75 changes as volcanic flows and hence ongoing volcanic activity on Venus. In line with that,
 76 recent estimates from scaling the volcanism of Earth to Venus yield 12 – 42 volcanic erup-
 77 tions on Venus in a year, depending on assumptions on the amount of volcanism asso-
 78 ciated with plume-induced subduction at coronae (Byrne & Krishnamoorthy, 2022; Van Zelst,
 79 2022). Future missions such as VERITAS (Smrekar et al., 2020) and EnVision (Ghail
 80 et al., 2016) will provide better constraints on Venus’s volcanic activity (Widemann et
 81 al., 2023, and references therein).

82 In the meantime, since Venus seems to be volcanically and geologically active, it
 83 is reasonable to assume that it is also seismically active. Indeed, its seismicity could be
 84 more extensive than that of Mars and the Moon, which are both believed to be signif-
 85 icantly less tectonically active than Venus (Stevenson et al., 2015). On these bodies, de-
 86 spite being in a stagnant lid regime, seismicity has been observed with the successfully
 87 deployed Apollo Lunar Surface Experiments Package on the Moon (Nakamura et al., 1982)
 88 and on Mars with the InSight mission (Banerdt et al., 2020). As Venus is now thought
 89 to be in a more tectonically active geodynamic regime than a stagnant lid (Rolf et al.,
 90 2022), its potential seismicity is thought to be at least comparable with Earth’s intraplate
 91 seismicity (Stevenson et al., 2015; Tian et al., 2023; Ganesh et al., 2023). On top of that,
 92 observed rift systems (Ivanov & Head, 2011), fold belts (Sabbeth et al., 2023b), wrin-
 93 kle ridges (Sabbeth et al., 2023b), and coronae features (Davaille et al., 2017; Gülcher
 94 et al., 2020) could be seismically active at present. There are even speculations that the
 95 Venera 14 lander recorded microseisms from far-away seismicity in the active Beta Re-
 96 gio on Venus, although there are many other potential explanations for these recorded
 97 signals (Ksanfomaliti et al., 1982).

98 Besides a large variety of tectonic features with potential Earth analogues, the crust
 99 of Venus has properties similar to the Earth’s crust. Considering their similarities is im-
 100 portant when assessing if seismicity might be governed by the same processes and there-
 101 fore manifest in the same manner in the two planets. Direct compositional measurements
 102 from the Soviet landers have shown that the surface of Venus has a similar composition
 103 to that of mid-oceanic ridge basalts on Earth (e.g., Abdrakhimov & Basilevsky, 2002).
 104 Moreover, the average crustal thickness of Venus has been estimated to be about 15 –
 105 20 km (James et al., 2013; Maia & Wiczeorek, 2022), which is comparable to the thick-
 106 ness of Earth’s oceanic crust. Considering these similarities, it is reasonable to use Earth’s
 107 seismic activity as a starting point to better understand the level of seismicity expected
 108 for Venus.

109 Here, we estimate upper and lower bounds of the amount of seismicity that could
 110 be expected for an active Venus, as well as an inactive Venus with seismicity reminis-
 111 cent of intraplate seismicity on Earth. By scaling the seismicity of the Earth to Venus
 112 in Section 2 for different tectonic settings, i.e., using the same philosophy as Byrne and
 113 Krishnamoorthy (2022) that Earth analogues can be applied to Venus, we obtain our re-
 114 sults (Section 3). We discuss the assumptions in our method and the estimates of pre-
 115 vious studies in detail in Section 4. This is followed by our conclusions in Section 5.

2 Methods

In order to make estimates of the seismicity of Venus, we use a global earthquake catalogue for Earth and sort the earthquakes into different tectonic areas on the globe, thereby obtaining an effective seismicity density for each tectonic setting. We then apply this same density to analogous Venusian settings to obtain three different possible estimates of Venus’s current seismicity: an estimate for an inactive Venus and an upper and lower bound for an active Venus, depending on the assumptions that we make. In this section, we present our methods in detail.

2.1 Tectonic settings on Earth

To obtain the seismicity density of different tectonic settings on Earth, we calculate the area of seven different tectonic settings on the Earth. For this, we use the recent maps of global geological provinces and tectonic plates from Hasterok et al. (2022). We define subduction and collision zone areas according to the zones of deformation defined by Hasterok et al. (2022), as the location of the seismicity associated with these types of plate boundaries typically encompasses a large, diffuse area. We extend the deformation zones of Hasterok et al. (2022) to account for deep earthquakes associated with subduction zones that lie outside of the deformation zones defined at the surface of the Earth. We further define the areas of transform and strike-slip regions, rift zones, and mid-oceanic ridges according to the mapping of Hasterok et al. (2022) by defining a 150 km wide band on either side of the respective plate boundary and correcting for overlapping areas. The remaining surface area of the Earth is divided into oceanic intraplate and continental intraplate regions, according to the mapped oceanic and continental crust by Hasterok et al. (2022). Hence, the surface area of the Earth is divided into seven distinct (non-overlapping) tectonic settings: subduction zones (5.13% of Earth’s surface area), collision zones (2.23%), transform and strike-slip regions (3.03%), rift zones (2.17%), mid-oceanic ridges (4.70%), and oceanic (50.44%) and continental intraplate (32.30%) regions (Figure 1a, Table S1).

2.2 Seismicity of the Earth

We use the global Centroid Moment Tensor (CMT; Dziewonski et al., 1981; Ekström et al., 2012) earthquake catalogue from 1976 – 2020 with a completeness magnitude of $M_w 5$ to characterise Earth’s annual seismicity. There are various methods to convert seismic moment M_0 (in N m) into moment magnitude M_w (e.g., Stein & Wysession, 2009; Beroza & Kanamori, 2015). Throughout our study, we follow Beroza and Kanamori (2015) by using the following expression:

$$\log M_0 = 1.5M_w + 9.05. \quad (1)$$

We sort the earthquakes of the CMT catalogue in the predefined tectonic areas (Figure 1b) and obtain an earthquake size-frequency distribution for the different tectonic settings (Figure 1c). The seismicity density for each of the tectonic settings found on Earth is then calculated by dividing the earthquake size-frequency distribution by the surface area (Figure 1d; Table S1).

Subduction zones have the highest seismicity density, followed by the other plate boundary settings and the overall global seismicity density of the Earth (Figure 1d). The seismicity density of collision zones and strike-slip regions are similar, with a slightly lower seismicity density for the rift zones. Intraplate seismicity clearly has the lowest seismicity density (approximately one order of magnitude less than the global seismicity density) with continental intraplate seismicity density being slightly higher than oceanic intraplate seismicity density.

162

2.3 Tectonic settings on Venus

163

164

165

166

167

168

169

170

171

172

173

For Venus, we consider three different tectonic settings in this study: Venusian rifts (chasmata), fold belts characterised by compressional deformation, and the volcano-tectonic corona features, for which we show representative examples in Figure 2 and their distribution on the surface of Venus in Figure 3a. For each of these tectonic settings, we assign plausible, potential Earth analogues to obtain an estimate of the potential annual seismicity of Venus. We refrain from including other tectonic settings found on Venus, such as tesserae and wrinkle ridges, as they do not have a clear Earth analogue, which makes their seismicity density unconstrained in our methodology. Instead, we consider the remaining area of Venus as an intraplate tectonic setting (Figure 3a). For a study on the potential seismicity of wrinkle ridges based on mapped fault lengths, see Sabbeth et al. (2023b), which is also discussed in Section 4.

174

2.3.1 Rift zones

175

176

177

178

179

180

181

182

183

184

Rifts on Venus are typically defined as large, broad structural units of 100 km or more that are characterised by closely-spaced extensional structures (Price & Suppe, 1995; Ivanov & Head, 2011). They are similar to the so-called groove belts on Venus, which are smaller and typically contain less dense faulting patterns (Ivanov & Head, 2011). The extensional features in rift zones are often interpreted as normal faulting and horst-and-graben structures, which are typically associated with continental rifting on Earth (Foster & Nimmo, 1996). Indeed, many studies have pointed out both the morphological similarity and the similar amount of crustal extension between rifts on Venus and continental rifts on Earth (e.g., McGill et al., 1981; R. Phillips et al., 1981; Stoddard & Jurdy, 2012).

185

186

187

188

189

190

For example, Foster and Nimmo (1996) provide a detailed comparison between the East African Rift system on Earth and the rift systems of Beta Regio on Venus. They identified many similarities, including maximum fault segment lengths, and concluded that differences stem from the lack of sediment and larger fault strength on Venus. As another example, Graff et al. (2018) suggested that the rift morphologies of Venus could be analogous to the Atlantic Rift System prior to ocean opening.

191

192

193

194

Modelling studies also indicate that continental rifting is a plausible mechanism to generate the rifting morphologies observed on Venus (Regorda et al., 2023). It is clear, however, that the difference in surface conditions between Venus and Earth plays a role in the rift mechanism as well (Regorda et al., 2023).

195

196

197

198

199

200

201

202

203

204

205

In general, the physical mechanisms governing the formation of rifts on Venus are still largely unclear. Continental rifting on Earth could be a reasonable analogue for Venus. However, considering Venus’s basaltic crustal composition — potentially more similar to Earth’s oceanic crust than its continental crust (Head, 1990) — and increased surface temperature, the rifts on Venus might also bear resemblance to the mid-oceanic ridges on Earth. Although they are both extensional processes, continental rifting and mid-oceanic ridge formation display quite different dynamics on Earth and consequently have different seismic signatures (Section 2.2). In addition, it is useful to note that rifts on Venus are commonly associated with regions suggested to be surface expressions of active mantle plumes, such as Atla, Beta, and Phoebe Regiones (Stofan et al., 1995; Kiefer & Peterson, 2003).

206

2.3.2 Fold belts

207

208

209

210

There are several different types of compressional structures on the surface of Venus, including ridges, ridge belts (defined as closely-clustered ridges; Frank & Head, 1990), and mountain belts (Price & Suppe, 1995). Here, we specifically focus on fold belts, defined by Price et al. (1996) as concentrated zones of compressive deformation forming

linear ridge belts analogous to terrestrial fold-and-thrust belts. As such, the mapping of fold belts by Price et al. (1996) also includes distinctly compressive regions, such as the mountain belt of Ishtar Terra. The various compressive features on Venus typically resemble each other, but differ in terms of topography (Ivanov & Head, 2011). The origin of these compressional features has been debated, with early studies proposing early stage mantle downwellings as a mechanism (Zuber, 1990) and perhaps even subduction (Kryuchkov, 1990). Here, we consider continental collision as the most appropriate analogue for fold belts on Venus (R. J. Phillips & Malin, 1984; Jull & Arkani-Hamed, 1995; Romeo & Turcotte, 2008).

2.3.3 *Coronae and corona-like features*

Coronae are roughly circular structures characterised by an annulus of high deformation (Price & Suppe, 1995). They are unique to Venus and are typically associated with volcanism and mantle upwellings (E. R. Stofan et al., 1992; Smrekar & Stofan, 1997). There are various topographic signatures associated with coronae, which have been linked to differences in formation mechanisms and stages of formation (Smrekar & Stofan, 1997; Gülcher et al., 2020). This variety in topographic signatures of coronae has inspired a variety in proposed formation mechanisms for coronae including hot spots followed by gravitational relaxation (E. R. Stofan et al., 1991), diapirs (Squyres et al., 1992; Koch & Manga, 1996; Musser Jr & Squyres, 1997), (deep) mantle plumes (Smrekar & Stofan, 1999; Schools & Smrekar, 2023), magmatic loading of the crust due to transient mantle plumes (Dombard et al., 2007), small-scale upwellings (Herrick, 1999; Johnson & Richards, 2003) and associated delamination (Smrekar & Stofan, 1997), gravitational relaxation of isostatically uncompensated plateaus potentially formed through diapirism (Janes et al., 1992), gravitational Rayleigh-Taylor lithosphere instabilities (Hoogenboom & Houseman, 2006), and lithospheric dripping as a result of the interaction between a mantle plume and a rift (Piskorz et al., 2014).

The formation of large coronae, such as Artemis corona, is typically associated with plume-lithosphere interactions where a rising plume impinges on the Venusian lithosphere and causes subduction-like dynamics and delamination at its edges (Schubert & Sandwell, 1995; Gerya, 2014; Davaille et al., 2017; Smrekar et al., 2018; Gülcher et al., 2020; Baes et al., 2021; Gülcher et al., 2023). For example, Gülcher et al. (2020) used 3-D numerical models to show that different corona structures could represent different plume styles and stages of formation with some coronae exhibiting subduction-like lithosphere dripping at their edges. Using these modelling insights and comparing to topographic data of Venus, Gülcher et al. (2020) found that 37 of 133 studied coronae (i.e., 27.8%) could be actively forming tectonic structures at present. The remaining coronae that they studied were either deemed to be inactive (26.3%) or inconclusive (45.9%) according to the modelled topography profiles. It is worth noting that the coronae studied in Gülcher et al. (2020) are not the complete set of observed coronae on Venus and are instead biased towards the larger corona structures with a diameter ≥ 300 km. Still, their modelling study provides compelling evidence that tectonic processes — and specifically subduction-like processes — could still be active today in a subset of the coronae.

In this study, we mainly follow Gülcher et al. (2020) in assuming that coronae are formed by subduction-like processes associated with plume-lithosphere interactions. Since this is likely only the case for a subset of coronae (e.g., Davaille et al., 2017), we also implicitly consider delamination or hot spot processes for corona formation (see Section 2.4.2 for more details).

2.3.4 *The surface areas of different tectonic features on Venus*

We calculate the surface area covered by rifts (8.25% of Venus’s surface area; Jurdry & Stoddard, 2007), coronae (7.76%), and fold belts (i.e., compressional regions; 1.64%)

261 from maps by Price and Suppe (1995); Price et al. (1996) as shown in Figure 3a (also
 262 see Table S2). We manually ensure that there are no overlapping regions by including
 263 rift-associated coronae as part of the rift system. The remaining surface area of Venus
 264 that is not assigned an actively-deforming tectonic setting is then considered to be in-
 265 traplate (82.35% of Venus’s surface; Figure 3a).

266 **2.4 Scaling from the Earth to Venus**

267 **2.4.1 Seismogenic thickness**

268 The seismogenic thickness of a planet’s lithosphere is the maximum depth at which
 269 earthquakes can nucleate, typically dictated by the temperature structure of the litho-
 270 sphere and the location of the brittle-ductile transition. Taken over the entire surface
 271 area of the planet, the seismogenic thickness transforms into the seismogenic volume.

272 On Earth, the down-dip limit of the seismogenic zone in subduction zones is es-
 273 timated to range from the 250°C to 550°C isotherms depending on the mineralogy (Tichelaar
 274 & Ruff, 1993; Peacock & Hyndman, 1999; He et al., 2007; Scholz, 2019). In a slightly
 275 narrower estimate, the down-dip limit of the seismogenic zone is typically associated with
 276 the 350°C and 450°C isotherms for megathrust seismicity (Hyndman & Wang, 1993; Hyn-
 277 dman et al., 1997; Gutscher & Peacock, 2003). In order to explain observations of intermediate-
 278 depth and deep seismicity in subduction zones and the existence of double seismic zones
 279 in subducted slabs, the 600°C and 800°C isotherms are also often cited as the factor lim-
 280 iting seismogenic thickness (Peacock, 2001; Yamasaki & Seno, 2003; Jung et al., 2004;
 281 McKenzie et al., 2005; Boettcher et al., 2007; Kelemen & Hirth, 2007; Wang et al., 2017).
 282 In high strain rate environments in tectonically active regions, earthquakes have been
 283 proposed to occur at temperatures up to 800°C (Chen & Molnar, 1983; Molnar, 2020).
 284 There have also been observations of earthquakes in continental lithosphere at depths
 285 modelled to correspond with isotherms of 750°C (Prieto et al., 2017) and earthquakes
 286 in slabs in regions estimated to exceed 1000°C (Melgar et al., 2018). In hotspot settings,
 287 such as Iceland, the average temperature at the base of the seismogenic zone has been
 288 estimated to be 750°C with a standard deviation of 100°C (Ágústsson & Flóvenz, 2005).
 289 Hence, estimates of the temperature defining the maximum seismogenic zone on Earth
 290 vary wildly and depend on the tectonic setting. Depending on the thermal structure of
 291 the lithosphere, the estimated seismogenic thickness therefore also carries a large uncer-
 292 tainty. In theoretical and modelling studies, the 600°C isotherm is often assumed to be
 293 the end-member temperature for brittle failure, and hence seismogenesis, in Earth’s litho-
 294 sphere for simplicity (Emmerson & McKenzie, 2007; Van Zelst et al., 2023).

295 As a measure of the amount of seismicity, the seismogenic thickness is of limited
 296 use as it merely defines the region where quakes could nucleate and slip. Indeed, earth-
 297 quakes can propagate below the seismogenic depth (e.g., Aderhold & Abercrombie, 2016),
 298 although they typically nucleate above it, and there are — depending on tectonic set-
 299 ting — vast regions with a significant seismogenic thickness that experience limited seis-
 300 micity, e.g. the interiors of continental plates, which typically undergo limited deforma-
 301 tion. However, despite its limitations, seismogenic thickness is still a useful variable to
 302 look at when determining the maximum amount of seismicity that could occur on a given
 303 planet.

304 Since Venus has a higher surface temperature than Earth, assuming the same seis-
 305 mogenic thickness for both planets is likely incorrect. More specifically, we expect Venus
 306 to have a lower seismogenic thickness than Earth due to its higher surface temperature
 307 and hence shallower brittle-ductile transition in its lithosphere. We therefore need to take
 308 the likely difference in seismogenic thickness between the two planets into account when
 309 estimating the seismicity of Venus.

310 In order to estimate the seismogenic thickness scaling factor between Earth and
 311 Venus, we first estimate the average seismogenic thickness for the Earth, which is rel-
 312 atively well constrained. For oceanic crust, we assume a representative seismogenic thick-
 313 ness of 36.5 km, which is the depth of the 600°C isotherm (McKenzie et al., 2005; Richards
 314 et al., 2018) for the average age of 64.2 Myrs of the oceanic crust (Seton et al., 2020).
 315 For an estimate of the average seismogenic thickness of continental crust, we follow Wright
 316 et al. (2013), who used coseismic and interseismic observations to arrive at estimates of
 317 14 ± 5 km and 14 ± 7 km of the average continental seismogenic thickness. Regional dif-
 318 ferences in seismogenic thickness are attributed to compositional differences, differing
 319 strain rates, or grain sizes, as Wright et al. (2013) found that there is no clear global re-
 320 lationship between seismogenic thickness and temperature structure for continental crust.
 321 So, using Wright et al. (2013)’s study, we assume a seismogenic thickness of 14 km for
 322 continental crust in our calculations. Then, applying the ratio of oceanic to continen-
 323 tal crust from Hasterok et al. (2022), we obtain an average seismogenic zone thickness
 324 for the Earth of 26.93 km.

325 For Venus, we calculate a likely minimum and maximum seismogenic thickness (see
 326 Van Zelst et al., 2024, for the data and scripts used in this study) from proposed end-
 327 member thermal gradients of Venus’s lithosphere (Smrekar et al., 2023; Bjonnes et al.,
 328 2021). Like for our Earth estimate, we calculate the depth corresponding to the 600°C
 329 isotherm, as this seems to limit the seismogenic zone on Earth most robustly. Seeing as
 330 Venus most likely has a drier interior than the Earth that is absent of volatiles, crustal
 331 rocks are stronger compared to their terrestrial counterparts (Mackwell et al., 1998). Hence,
 332 brittle deformation could also occur up to deeper isotherms in Venus’s interior. There-
 333 fore, we also provide seismogenic thickness estimates assuming a temperature of 800°C
 334 as the limiting factor in Van Zelst et al. (2024). However, for consistency with the es-
 335 timate for Earth’s seismogenic thickness, we chose the 600°C isotherm to compute the
 336 values in our analysis for Venus. To obtain a minimum estimate of Venus’s seismogenic
 337 zone thickness, we calculate the average thermal gradient for Venusian rifts estimated
 338 by Smrekar et al. (2023), which results in a seismogenic thickness of 7.3 km (Van Zelst
 339 et al., 2024) assuming a limiting temperature of 600°C. As a maximum estimate, we use
 340 the proposed minimum thermal gradient of 6 K/km for the Mead crater on Venus by Bjonnes
 341 et al. (2021), which results in a seismogenic thickness of 22.7 km (Van Zelst et al., 2024)
 342 for a temperature of 600°C at the base of the seismogenic zone. We note that these es-
 343 timates represent the thermal gradients during the formation of the associated features,
 344 but given the young ages predicted for Venus’s surface these values are likely represen-
 345 tative for its current thermal state.

346 Combining these estimates of the Venusian seismogenic thickness with that of Earth,
 347 we obtain minimum and maximum scaling ratios of 0.27 and 0.84, respectively, to ac-
 348 count for the likely difference in seismogenic thickness between Venus and Earth.

349 ***2.4.2 Three end-member estimates***

350 We consider three different scenarios when scaling the seismicity from the Earth
 351 to Venus (Table S3). First, we consider an inactive Venus where the only seismicity on
 352 the planet is a background seismicity similar to the continental intraplate seismicity on
 353 Earth. This minimum level of seismicity on Venus is a popular hypothesis that has been
 354 used by other studies as well (e.g., Stevenson et al., 2015; Tian et al., 2023; Ganesh et
 355 al., 2023). Here we obtain this estimate by scaling the entirety of Venus with continen-
 356 tal intraplate seismicity on Earth.

357 As a second estimate, we consider an active Venus with conservative assumptions
 358 on its level of activity to provide a lower bound. Following Davaille et al. (2017); Gülcher
 359 et al. (2020); Byrne and Krishnamoorthy (2022), we assume that coronae are surface ex-
 360 pressions of plume-lithosphere interactions with subduction-like features and therefore

361 have a seismic signature similar to that of Earth’s subduction zones. However, for this
 362 lower bound estimate, we do not consider the entire corona area to be active subduction-
 363 like features and associated with the high seismicity density of subduction zones. Instead,
 364 we assume that 27.8% of the area of coronae is active according to Gülcher et al. (2020)
 365 and we only scale this area with subduction zones on Earth. The remaining area of the
 366 coronae is scaled with continental intraplate seismicity on Earth. Hence, we effectively
 367 assume that the corona formation mechanism for the remaining coronae is more akin to
 368 seismicity associated with hot spots or delamination processes on Earth, whose seismic
 369 signatures are implicitly included in our continental and oceanic intraplate seismic den-
 370 sities for Earth. We further assume that the rift zones on Venus have seismicity simi-
 371 lar to (continental) rift zones on Earth (S. Solomon, 1993; Foster & Nimmo, 1996; Basilevsky
 372 & McGill, 2007; Harris & Bédard, 2015; Graff et al., 2018). The observed fold belts on
 373 Venus that we assume to be compressional features are assumed to have a similar seis-
 374 micity signature to collision zones on Earth. Like the inactive Venus scenario, the remain-
 375 ing area of Venus is scaled according to continental intraplate seismicity on Earth.

376 Our third and last estimate is for an active Venus with the most liberal assump-
 377 tions of plausible tectonic activity on Venus. In this estimate, we assume that all coro-
 378 nae are active, since the amount of active coronae is still highly uncertain (Gülcher et
 379 al., 2020). So, we scale the entire corona area with the subduction seismicity of the Earth.
 380 For the rift zones on Venus, we now scale the seismicity with mid-oceanic ridge seis-
 381 micity on Earth, instead of continental rifting (Graff et al., 2018). Like our lower bound es-
 382 timate for active Venus, we scale the area of fold belts on Venus with collision zones on
 383 Earth and we assume that the rest of the planet is equivalent to continental intraplate
 384 seismicity on Earth.

385 Combining the scaling for the seismogenic zone thickness (Section 2.4.1) with the
 386 three scalings based on the tectonic features allows us to arrive at three different end-
 387 member seismicity estimates for Venus. In short, we obtain the global amount of annual
 388 venusquakes for a certain magnitude $N_{\text{vq}|M_w}$ by applying the following equation:

$$N_{\text{vq}|M_w} = f_{\Delta D} \sum_{\text{tectonic features}} A_{t,V} \cdot \frac{N_{\text{eq},t|M_w}}{A_{t,E}} \quad (2)$$

389 where $f_{\Delta D}$ is the seismogenic zone scaling factor (i.e., 0.27 and 0.84); $A_{t,V}$ is the sur-
 390 face area A of a tectonic feature t on Venus V ; $N_{\text{eq},t|M_w}$ is the number of annual earth-
 391 quakes for a given analogous Earth tectonic feature at a given moment magnitude; and
 392 $A_{t,E}$ is the corresponding surface area of the analogous tectonic feature on Earth. The
 393 sum then indicates a summation over all the tectonic features that are scaled on Venus,
 394 up to and including the intraplate regions, such that we sum over the entire surface area
 395 of Venus. Scaling with the seismogenic thickness as well as the areas of the tectonic set-
 396 tings, effectively allows us to scale by seismogenic volume per tectonic setting to obtain
 397 estimates for Venus’s seismicity (Table S3).

398 **2.4.3 Extrapolating to other magnitudes**

399 In order to actually calculate the potential amount of venusquakes and to extrap-
 400 olate to earthquake magnitudes below the completeness magnitude of $M_w 5$ of the CMT
 401 catalogue, we effectively scale the average slopes of the size-frequency distribution for
 402 the different tectonic settings on Earth (equivalent to $N_{\text{eq},t}$ for all moment magnitudes;
 403 Figure 1c). We specifically assume that the size-frequency distribution of medium-sized
 404 earthquakes with a seismic moment of 10^{17} N m to 10^{19} N m is representative for the
 405 size-frequency distribution of smaller earthquake magnitudes, i.e., the earthquakes fol-
 406 low Gutenberg-Richter statistics (Gutenberg & Richter, 1956; Beroza & Kanamori, 2015).
 407 This assumption allows us to provide estimates of the amount of venusquakes with mo-

408 ment magnitudes of $M_w 3$ and $M_w 4$. We refrain from reporting on the amount of venusquakes
 409 with lower magnitudes, because they are unlikely to be detected in future seismological
 410 exploration missions of Venus (Krishnamoorthy et al., 2020; Brissaud et al., 2021).

411 Calculating the amount of large venusquakes with magnitudes $\geq M_w 8$ is less straight-
 412 forward, as the (potential) maximum quake magnitude on Venus is unknown. One con-
 413 tributing factor is the lower seismogenic thickness of Venus compared to Earth (Section 2.4.1),
 414 which affects the maximum magnitude of quakes in addition to the frequency of events.
 415 However, there is limited data for Earth on earthquakes with magnitudes $\geq M_w 8$, be-
 416 cause of their large recurrence time (Figure 1). For these reasons, we do not explicitly
 417 comment on the occurrence of quakes $\geq M_w 8$ on Venus in this study, although our method-
 418 ology does provide estimates (e.g., Figure 3).

419 3 Results

420 Our results for the different Venus scenarios are summarised in Figure 3 and Ta-
 421 ble 1, 2, where we list the estimated annual number of quakes for a given moment mag-
 422 nitude and the global seismicity densities on Venus for our different estimates.

423 3.1 Inactive Venus

424 In our first estimate, we assume that the entirety of Venus can be scaled with the
 425 continental intraplate seismicity of the Earth, so the global estimate and the intraplate
 426 estimate overlap perfectly in Figure 3b. As expected, the amount of seismicity in this
 427 scenario is significantly less than that on Earth with 95 – 296 venusquakes $\geq M_w 4$ es-
 428 timated annually, compared to 12,207 earthquakes $\geq M_w 4$ per year on Earth. The as-
 429 sociated seismicity density for quakes $\geq M_w 4$ lies between $0.21 \cdot 10^{-6}$ and $0.64 \cdot 10^{-6}$ year $^{-1}$ km $^{-2}$
 430 (Table 2), which is on the same order of magnitude as that of intraplate seismicity on
 431 Earth.

432 3.2 Active Venus - lower bound

433 The lower bound for our active Venus estimate globally predicts more seismicity
 434 than the inactive, intraplate Venus estimate (Section 3.1). The fold belt, rift, and intraplate
 435 tectonic settings on Venus have seismicity on the same order of magnitude in this esti-
 436 mate, as shown by the overlapping bands of seismicity in Figure 3c (also see Figure S1).
 437 The coronae have an order of magnitude more seismicity associated with them, although
 438 only 27.8% of them are assumed to have a subduction-like seismicity density in this es-
 439 timate. Summing up the seismicity of the different tectonic settings results in estimates
 440 of 1,161 – 3,609 venusquakes per year with a moment magnitude $\geq M_w 4$ and a seismic-
 441 ity density of $2.52 \cdot 10^{-6}$ to $7.84 \cdot 10^{-6}$ year $^{-1}$ km $^{-2}$ globally for venusquakes $\geq M_w 4$ (Ta-
 442 ble 2). This global seismicity density is significantly less than that of the Earth or any
 443 of its plate boundary settings.

444 3.3 Active Venus - upper bound

445 The upper bound of estimated seismicity for an active Venus (Figures 3d, S2) is
 446 very close to – and even slightly larger than – the annual seismicity observed on Earth,
 447 primarily due to the scaling of coronae with Earth’s subduction zone seismicity in this
 448 estimate, which also dominates Earth’s seismicity (Figure 1c). Since we scale the rifts
 449 on Venus with Earth’s mid-oceanic ridge seismicity in this estimate, we have a different
 450 slope for Venusian rift seismicity. This results in an increase in smaller quakes with $M_w \leq$
 451 5. There is no difference between the seismicity expected for the fold belt tectonic set-
 452 ting compared to the lower bound for an active Venus (Section 3.2), as it is scaled in the
 453 same way.

| Estimate | $M_w \geq 3.0$ | $M_w \geq 4.0$ | $M_w \geq 5.0$ | $M_w \geq 6.0$ | $M_w \geq 7.0$ |
|----------------------------|----------------|----------------|----------------|----------------|----------------|
| Inactive Venus | 826 - 2568 | 95 - 296 | 11 - 34 | 1 - 4 | 0 - 0 |
| Active Venus - lower bound | 10760 - 33460 | 1161 - 3609 | 126 - 391 | 14 - 42 | 2 - 5 |
| Active Venus - upper bound | 84263 - 262023 | 5715 - 17773 | 465 - 1446 | 44 - 136 | 4 - 15 |

Table 1. Number of venusquakes per year equal to or larger than a certain moment magnitude for our three possible Venus scenarios. A range is provided based on the uncertainties in the chosen scaling factor for the seismogenic thickness.

454 Globally, we then estimate 5,715 – 17,773 venusquakes of moment magnitude $\geq M_w 4$,
 455 with the upper bound being larger than the number of $M_w \geq 4$ earthquakes estimated
 456 for the Earth (12,207). The seismicity density of quakes $M_w \geq 4$ varies from $12.42 \cdot 10^{-6}$
 457 to $38.62 \cdot 10^{-6}$ year⁻¹ km⁻² (Table 2). This lowest possible seismicity density for an up-
 458 per bound to our active Venus estimate is slightly lower than the Earth’s seismicity den-
 459 sity for continental rift zones ($16.98 \cdot 10^{-6}$ year⁻¹ km⁻²) and the highest possible seis-
 460 micity density is larger than that of the seismicity density of collision settings on the Earth
 461 ($33.62 \cdot 10^{-6}$ year⁻¹ km⁻²) (Table S1).

462 4 Discussion

463 In this study, we provide three end-member estimates of possible Venusian seismic-
 464 ity by looking at Earth analogues, following the same philosophy of Byrne and Krish-
 465 namoorthy (2022) who previously applied this logic to determine the frequency of vol-
 466 canic eruptions on Venus. In contrast to Byrne and Krishnamoorthy (2022), we calcu-
 467 late the seismic densities for individual tectonic settings and then scale according to their
 468 surface areas and appropriate Earth analogues.

469 Generally, we estimate that the seismicity of Venus is lower than that of the Earth,
 470 except for the most active end-member of Venus activity. Indeed, there are large differ-
 471 ences between the various estimates, indicating a range of possible seismic activity on
 472 Venus at present, depending on the many assumptions we are forced to make given the
 473 limited amount of data from Venus.

474 4.1 Likely causes of differences between the seismicity on Earth and Venus

475 Before we assess the individual assumptions we made to obtain our different esti-
 476 mates of Venusian seismicity, it is useful to assess the overarching assumption that Earth’s
 477 seismicity can be scaled to Venus.

478 One of the biggest and most straightforward differences between the Earth and Venus
 479 is their different surface temperature. Since temperature plays a crucial role in seismic-
 480 ity through its control on the brittle-ductile transition (Tichelaar & Ruff, 1993; Hynd-
 481 man et al., 1997; Peacock & Hyndman, 1999; Gutscher & Peacock, 2003; Scholz, 2019),
 482 it will have a large effect on the amount of seismicity that can occur. On a global scale,
 483 different surface temperatures can result in different tectonic regimes and deformation
 484 mechanisms (Lenardic et al., 2008; Foley et al., 2012; Weller et al., 2015) which could
 485 greatly change the seismic signatures. In its most extreme case some studies argue that
 486 there will be little to no seismicity on Venus, at least at higher magnitudes (e.g., Karato
 487 & Barbot, 2018). These studies argue that the high surface temperatures on Venus may
 488 exclude the possibility of any kind of substantial seismogenic zone and the unstable slip
 489 mechanisms responsible for earthquakes. Instead, the stresses that are built up in the
 490 Venusian lithosphere could be released through aseismic processes, such as creep (sta-
 491 ble slip) and viscous flow. Karato and Barbot (2018) arrive at this conclusion by assum-

| Tectonic setting | Minimum seismicity density ($\cdot 10^{-6}$ year $^{-1}$ km $^{-2}$) | Maximum seismicity density ($\cdot 10^{-6}$ year $^{-1}$ km $^{-2}$) |
|----------------------------|--|--|
| Inactive Venus | 0.21 | 0.64 |
| Active Venus - lower bound | 2.52 | 7.84 |
| Active Venus - upper bound | 12.42 | 38.62 |

Table 2. Estimated minimum and maximum seismicity densities on Venus for quakes $\geq M_w 4$ for three scenarios with different activity-level assumptions.

492 ing a crustal thickness of 30 km based on a global stagnant lid regime and a limit of the
493 seismicogenic zone in the crust at the 400°C isotherm and in mantle at 600°C. However,
494 recent estimates of the average crustal thickness of Venus are 15 - 20 km (James et al.,
495 2013; Maia & Wiczorek, 2022). Additionally, strictly separating the mechanical behaviour
496 of the crust and mantle like this is unrealistic. Instead, a better approach might be to
497 look at the behaviour of the lithosphere as a whole. For oceanic lithosphere the limit-
498 ing temperatures for the deepest quakes are the 600 - 800°C isotherms (Chen & Mol-
499 nar, 1983). Applying these assumptions instead, the method of Karato and Barbot (2018)
500 does predict a thin seismicogenic thickness with the possibility for quakes on Venus.

501 In contrast to this, there are also studies that cite the high surface temperature on
502 Venus as a potential indirect source of quakes on Venus. Lognonné and Johnson (2015)
503 mention that the rising surface temperature throughout Venus’s evolution could gener-
504 ate compressive thermoelastic stresses in the crust (S. C. Solomon et al., 1999; Dragoni
505 & Piombo, 2003). This increase in compressive stress could in turn form or activate re-
506 verse faults in Venus’s lithosphere. Comparing to the Earth analogues of regions with
507 compressive faulting, Lognonné and Johnson (2015) suggest that these stresses could lead
508 to quakes with a maximum moment magnitude of 6.5.

509 In our estimates, we have taken the difference in surface temperatures and its ef-
510 fect on seismicity into account through scaling end-member estimates of the seismicogenic
511 thickness of Venus with the average seismicogenic thickness of Earth. While this is not a
512 perfect solution that encapsulates the complexity of the effect of increased surface tem-
513 peratures, this at least forms a first approximation to take this difference into account.

514 Another important difference between Venus and Earth is likely to be the amount
515 of water available in the crust. On Earth, water plays a vital role, especially in subduc-
516 tion seismicity, with the pore-fluid pressure crucial in determining the stresses in megath-
517 rust settings (Seno, 2009; Angiboust et al., 2012) and dehydration reactions responsi-
518 ble for intermediate-depth and deep seismicity in subduction zones (Green & Houston,
519 1995; Hacker et al., 2003; Jung et al., 2004; Houston, 2015; Wang et al., 2017). This wa-
520 ter is typically added to the subduction system at the outer rise that underlies an ocean
521 in subduction zones (Boneh et al., 2019). On Venus, the amount of water in the litho-
522 sphere is relatively unconstrained (Gillmann et al., 2022; Rolf et al., 2022), with some
523 studies suggesting that Venus is currently relatively dry (Grinspoon, 1993; Namiki & Solomon,
524 1998; Smrekar & Sotin, 2012; Salvador et al., 2022), while others argue that there might
525 still be a significant amount of water in Venus’s mantle (Gillmann et al., 2022). This makes
526 it highly uncertain how big a role water could play in the seismicity of Venus. Our es-
527 timates encompass the full spectrum of possible seismicity on Venus with our lower bound
528 using Earth’s intraplate seismicity, where water likely plays a smaller role, and our up-
529 per bound including subduction seismicity, where water is an important factor.

530 Strain rates play an important role in seismicity as well, because they determine
 531 the time scale of stress build-up and the recurrence time of earthquakes. On Venus, strain
 532 rates similar to Earth’s active margins have been suggested by R. E. Grimm (1994). How-
 533 ever, due to the lack of Earth-like plate tectonics and plate boundaries, there are over-
 534 all potentially less large rupture areas, leading to less large-magnitude quakes on Venus.
 535 The decreased seismogenic thickness of Venus also plays a role in this by limiting the max-
 536 imum rupture area. Although our estimates provide a range of potential venusquakes
 537 at large magnitudes (Table 1), it is therefore uncertain if large venusquakes could actu-
 538 ally occur. Preliminary mission designs suggest that quake magnitudes of $M_w \geq 3$ could
 539 be feasibly observed by a range of plausible seismic detection methods (Krishnamoorthy
 540 et al., 2020; Brissaud et al., 2021) and our estimates are likely most plausible for this range
 541 of seismic magnitude $3 \leq M_w \leq 5$.

542 All in all, there are many uncertainties when it comes to estimating the seismic-
 543 ity of Venus from Earth’s seismicity. Higher resolution data and missions focused on ob-
 544 serving seismicity (discussed in Section 4.3) will help to obtain seismicity estimates for
 545 Venus independent of Earth. However, since those constraints are not yet available, scal-
 546 ing the seismicity of the Earth is a reasonable first-order approximation to gain some in-
 547 sights into the potential seismicity of Venus.

548 4.2 Assumptions in and limitations of our seismicity estimates

549 For our inactive Venus estimate, we assume that the global background seismic-
 550 ity of Venus is similar to the continental intraplate seismicity of the Earth. This is a com-
 551 mon assumption that has also been suggested by e.g., Lorenz (2012); Stevenson et al.
 552 (2015); Byrne et al. (2021); Tian et al. (2023). The number of venusquakes $\geq M_w 4$ per
 553 year for this estimate (95 – 296) is also the same order of magnitude as the estimate of
 554 Ganesh et al. (2023), who calculate an estimate of Venus’s seismicity based on the cool-
 555 ing of the planet and the corresponding contraction of the lithosphere and thereby pre-
 556 dict ~ 265 venusquakes $\geq M_w 4$ per year. Lognonné and Johnson (2015) mention that
 557 E. Stofan et al. (1993) arrive at a slightly higher estimate of 100 quakes $\geq M_w 5$ per year
 558 for intraplate activity with a strain rate of 10^{-19} s^{-1} (R. Grimm & Hess, 1997). In com-
 559 parison, we estimate 11 – 34 quakes $\geq M_w 5$ per year. The reason for this discrepancy
 560 is that E. Stofan et al. (1993) assume a thicker seismogenic layer (30 km) than we do.

561 Of course, we cannot completely exclude a completely inactive Venus with seismic-
 562 ity densities even lower than our inactive Venus estimate. So, if future missions (Section 4.3)
 563 would find less than 95 quakes $\geq M_w 4$ per year, this would indicate that either the pro-
 564 cesses that are responsible for creating intraplate seismicity on the Earth do not oper-
 565 ate on Venus or the seismic moment release on Venus is fundamentally slower on Venus
 566 than on Earth. Physically, this lower seismic activity could for example be caused by the
 567 slower cooling of Venus than previously thought, thereby decreasing the amount of quakes
 568 predicted by Ganesh et al. (2023).

569 For our estimates for an active Venus, we scale the areas of fold belts associated
 570 with compressional deformation on Venus with the seismicity of collision zones on Earth.
 571 We believe this to be a reasonable assumption, considering that Venus’s fold belts and
 572 the Earth analogue are both compressional regimes. The rifts on Venus are scaled with
 573 continental rift seismicity on Earth in the lower bound estimate for an active Venus. This
 574 is also a reasonable assumption, with many studies pointing to the morphological and
 575 geological similarities between the rift zones on Venus and continental rifts on Earth such
 576 as the East African rift zone (S. Solomon, 1993; Foster & Nimmo, 1996; Kiefer & Swaf-
 577 ford, 2006; Basilevsky & McGill, 2007; Stoddard & Jurdy, 2012; Graff et al., 2018; Re-
 578 gorda et al., 2023). For our upper bound, we scale the rift zones of Venus with mid-oceanic
 579 ridge seismicity since it is also an extensional setting and the higher temperatures at the
 580 mid-oceanic ridges and the corresponding different slope of the size-frequency distribu-

581 tion on Earth might be a better fit for rift seismicity under Venus’s high surface tem-
 582 perature. On Earth, the different seismic signatures between continental rifts and mid-
 583 oceanic ridges is not purely temperature-related. Instead, the inherent tectonic differ-
 584 ences between the two settings plays a role as well. Since it is unclear which of these two
 585 physical mechanisms (or their seismic signatures) best represents the rifting processes
 586 of Venus, we believe using one of them in the lower bound estimate and one in the up-
 587 per bound estimate catches the uncertainty in governing mechanisms in our estimates.
 588 For the coronae, we scale with subduction, since multiple studies suggest that coronae,
 589 or at least a subset of them, could be the surface expressions of plume-lithosphere in-
 590 teractions with subduction-like features (Davaille et al., 2017; Gülcher et al., 2020; Byrne
 591 & Krishnamoorthy, 2022). However, the seismicity associated with this type of plume-
 592 lithosphere interactions is uncertain. Assigning the same seismicity density as regular
 593 subduction processes on Earth follows Gülcher et al. (2020) and is a reasonable first-order
 594 approximation in the absence of other constraints, although the presumable lack of wa-
 595 ter in coronae and the higher surface temperature will certainly affect its seismic signa-
 596 ture as well. Future modelling studies that combine geodynamic modelling with seismic
 597 cycle modelling and dynamic ruptures (e.g., van Dinther, Gerya, Dalguer, Mai, et al.,
 598 2013; van Dinther, Gerya, Dalguer, Corbi, et al., 2013; van Dinther et al., 2014; Van Zelst
 599 et al., 2019) are needed to assess the seismic signatures that could be expected at Venu-
 600 sian coronae. In the interest of providing an upper and lower bound, scaling the coro-
 601 nae by activity is a good first order approximation. However, it is also possible that coro-
 602 nae seismicity does not scale with Earth’s subduction seismicity, but is instead more anal-
 603 ogous to, for example, rift or transform fault seismicity, as suggested for the center of
 604 Artemis corona (Spencer, 2001). In general though, our upper bound for Venusian seis-
 605 micity results in seismicity levels slightly higher than, but similar to, that of the Earth,
 606 which has also already been suggested previously (e.g., Lorenz, 2012). Choosing a dif-
 607 ferent seismicity density for coronae, such as that of the transform fault setting, would
 608 result in a lower amount of estimated venusquakes. Since we are attempting to provide
 609 an upper limit to the possible amount of annual venusquakes, our assumption of a sub-
 610 duction seismicity density is reasonable.

611 Apart from the uncertainty in scaling the chosen tectonic settings correctly, there
 612 are also tectonic settings on Venus that we neglect to scale explicitly. For example, we
 613 do not explicitly scale the tesserae of Venus with a tectonic setting on Earth, although
 614 they are implicitly scaled with the background intracontinental seismicity of the Earth.
 615 This is arguably one of the most reasonable assumptions for tesserae, considering that
 616 prevailing hypotheses include that they are continental crust analogues (Romeo & Tur-
 617 cotte, 2008; M. Gilmore et al., 2015). We also do not consider the observed extensive re-
 618 gions of wrinkle ridges as seismically active beyond the background intracontinental seis-
 619 micity of the Earth. A recent study by Sabbeth et al. (2023a) presented a conservative
 620 estimate of $9.1 \cdot 10^{16}$ N m to $5.1 \cdot 10^{17}$ N m per year for the annual moment release for
 621 wrinkle ridges on Venus based on (low-resolution) mapped fault lengths. Assuming a max-
 622 imum quake size on Venus of $M_w 4$, this translates to 81 to 455 wrinkle ridge quakes $M_w \leq$
 623 4 on Venus per year. This is a similar amount of $M_w \leq 4$ quakes as predicted for the
 624 intraplate, fold belt, and rift settings in our three different estimates ranging from in-
 625 active to active. Beyond tesserae and wrinkle ridges, there are also other kinds of defor-
 626 mation structures and potential seismic sources that are not considered in this study, such
 627 as densely fractured plains, that could also contribute significantly to the seismicity of
 628 Venus.

629 Note that in the estimates presented here, only one type of seismic source is con-
 630 sidered, i.e. earthquakes, which by definition are associated with tectonics and volcan-
 631 ism. Other sources such as landslides (Pavri et al., 1992; M. Bulmer & Guest, 1996; M. Bul-
 632 mer et al., 2006; M. H. K. Bulmer, 2012; Hahn & Byrne, 2023) could be responsible for
 633 seismic signals on Venus as well.

634

4.3 Determining the actual seismicity of Venus in the future

635

636

637

638

639

In the next decade, VERITAS (Smrekar et al., 2020) and EnVision (Ghail et al., 2016) will provide a wealth of new data, including high resolution topography, that will provide better constraints on the actual lengths, offsets, and displacements of Venusian faults. This will provide another basis of estimating Venus’s seismicity through scaling relationships applied to surface fault observations (Sabbeth et al., 2023a, 2023b).

640

641

642

643

644

645

646

647

648

649

The new Venus missions will also indirectly provide stronger constraints on the seismogenic thickness, which is typically deduced from thermal gradients estimated from studies of the elastic and mechanical lithosphere thickness (e.g. Anderson & Smrekar, 2006; Borrelli et al., 2021; Maia & Wieczorek, 2022; Smrekar et al., 2023) or from impact crater modeling (Bjonnes et al., 2021). These studies rely on the analysis of gravity and topography data, for which a higher resolution will become available from the VERITAS (Smrekar et al., 2020) and EnVision (Ghail et al., 2016) missions. Estimates of the thermal gradient and associated seismogenic thickness could then be obtained with a higher accuracy and on a more global scale than currently available. They could be included in future studies of seismicity on Venus and improve on the estimates presented here.

650

651

652

653

654

655

Most importantly though, VERITAS will be able to directly measure surface deformation through Repeat Pass Interferometry (RPI) at 2 mm height precision (Smrekar et al., 2020). EnVision will most likely also be able to measure surface deformation, although to a more limited extent. Besides quantifying movements on the surface of Venus for the first time, both missions will also qualitatively provide insights into which regions are geologically and potentially seismically active.

656

657

658

659

660

Until the era of new Venus data, we are unfortunately limited by the currently-available data of Venus. The simplest, first-order estimate of the seismicity of Venus is therefore obtained here through scaling Earth analogues to Venus, without considering individual fault lengths or displacements and detailed seismogenic thickness estimates and instead uses the seismicity density characteristics of different tectonic settings on Earth.

661

662

663

664

665

666

667

668

669

670

To distinguish between the different scenarios presented in this study and determine how seismically active Venus is, a seismological or geophysical mission to Venus is required to measure seismic signals. Although the NASA- and ESA-selected missions to Venus currently do not focus on this, there are promising proposals to measure Venus’s seismicity in the not-too-distant future. For example, Kremic et al. (2020) presented a mission proposal for a long-duration Venus lander with a seismometer on board that can withstand Venus’s high surface temperature. In addition, recent advances in the balloon-detection of earthquakes show great promise for applications to Venus (Garcia et al., 2022; Krishnamoorthy & Bowman, 2023). Our estimates for Venusian seismicity may help guide the design of these missions.

671

5 Conclusions

672

673

674

675

676

677

678

679

680

681

682

We estimate upper and lower bounds on the expected annual seismicity of Venus by scaling the seismicity of the Earth to Venus according to the surface area of different tectonic settings and the difference in seismogenic thickness between the two planets. Our most conservative estimate is an ‘inactive Venus’, where we assume that the global seismicity of Venus is comparable to Earth’s continental intraplate seismicity. This results in 95 – 296 venusquakes $\geq M_w4$ per year depending on the assumption of seismogenic zone thickness. For our active Venus scenarios, we assume that the rifts, fold belts, and coronae on Venus are seismically active. For a lower bound on an active Venus, we then find 1,161 – 3,609 venusquakes $\geq M_w4$ annually, which increases to 5,715 – 17,773 venusquakes $\geq M_w4$ for assumptions that constitute our most active Venus scenario. This latter scenario is slightly larger than the seismic activity level of the Earth. Future

683 seismological and geophysical missions could measure the actual seismicity of Venus and
 684 distinguish between our three proposed end-members of Venusian seismic activity.

685 Acknowledgements

686 We warmly thank the editor Laurent Montési and reviewers Sue Smrekar and Joseph
 687 O'Rourke who provided thorough and constructive feedback. We also thank two anony-
 688 mous reviewers who provided feedback on an earlier version submitted to GRL. This re-
 689 search is supported by the International Space Science Institute (ISSI) in Bern, Switzer-
 690 land through ISSI International Team project #566: Seismicity on Venus: Prediction &
 691 Detection. The authors warmly thank the entire ISSI team for fruitful discussions and
 692 feedback. IvZ, JM, ACP, and MS additionally acknowledge the financial support and en-
 693 dorsement from the DLR Management Board Young Research Group Leader Program
 694 and the Executive Board Member for Space Research and Technology. IvZ also grate-
 695 fully acknowledges the support by the Deutsche Forschungsgemeinschaft (DFG, German
 696 Research Foundation), Project-ID 263649064 - TRR 170.

697 Author contribution statement

698 Conceptualization: Iris van Zelst
 699 Data curation: Julia Maia, Richard Ghail, Moritz Spühler
 700 Formal Analysis: Iris van Zelst, Julia Maia
 701 Funding acquisition: Iris van Zelst, Ana-Catalina Plesa
 702 Methodology: Iris van Zelst, Richard Ghail
 703 Supervision: Iris van Zelst
 704 Visualization: Iris van Zelst, Julia Maia
 705 Writing – original draft: Iris van Zelst
 706 Writing – review & editing: Iris van Zelst, Julia Maia, Richard Ghail, Ana-Catalina
 707 Plesa, Moritz Spühler

708 Data availability statement

709 The Jupyter Notebooks used to make the results and plot the figures as well as the
 710 CMT database and geospatial vector data (shapefiles) of the tectonic setting areas on
 711 Earth can be found in Van Zelst et al. (2024). Explanations of individual files in this repos-
 712 itory and additional figures and tables are provided in the Supplementary Material. Fig-
 713 ures were made with Python in Jupyter Notebooks and Adobe Illustrator. We used the
 714 colourblind-friendly colour map from the IBM Design Library (David Nichols, 2022; re-
 715 trieved: February 16, 2023).

716 References

- 717 Abdrakhimov, A., & Basilevsky, A. (2002). Geology of the Venera and Vega landing-
 718 site regions. *Solar System Research*, *36*, 136–159.
 719 Aderhold, K., & Abercrombie, R. E. (2016). Seismotectonics of a diffuse plate
 720 boundary: Observations off the sumatra-andaman trench. *Journal of Geophysi-
 721 cal Research: Solid Earth*, *121*(5), 3462–3478.
 722 Ágústsson, K., & Flóvenz, Ó. G. (2005). The thickness of the seismogenic crust
 723 in iceland and its implications for geothermal systems. In *Proceedings of the*

- 724 *world geothermal congress* (pp. 24–29).
- 725 Anderson, F. S., & Smrekar, S. E. (2006). Global mapping of crustal and litho-
726 spheric thickness on Venus. *Journal of Geophysical Research: Planets* (1991–
727 2012), 111(E8).
- 728 Angiboust, S., Wolf, S., Burov, E., Agard, P., & Yamato, P. (2012). Effect of fluid
729 circulation on subduction interface tectonic processes: Insights from thermo-
730 mechanical numerical modelling. *Earth and Planetary Science Letters*, 357,
731 238–248.
- 732 Baes, M., Stern, R. J., Whattam, S., Gerya, T. V., & Sobolev, S. V. (2021). Plume-
733 induced subduction initiation: Revisiting models and observations. *Frontiers in*
734 *Earth Science*, 9, 766604.
- 735 Banerdt, W. B., Smrekar, S. E., Banfield, D., Giardini, D., Golombek, M., Johnson,
736 C. L., ... others (2020). Initial results from the InSight mission on Mars.
737 *Nature Geoscience*, 13(3), 183–189.
- 738 Basilevsky, A. T., & McGill, G. E. (2007). Surface evolution of Venus. *Exploring*
739 *Venus as a terrestrial planet*, 176, 23–43.
- 740 Beroza, G., & Kanamori, H. (2015). 4.01 - Earthquake Seismology: An Introduction
741 and Overview. In G. Schubert (Ed.), *Treatise on geophysics* (Second ed., p. 1 -
742 50). Oxford: Elsevier.
- 743 Bjornnes, E., Johnson, B., & Evans, A. (2021). Estimating Venusian thermal condi-
744 tions using multiring basin morphology. *Nature Astronomy*, 5(5), 498–502.
- 745 Boettcher, M. S., Hirth, G., & Evans, B. (2007). Olivine friction at the base of
746 oceanic seismogenic zones. *Journal of Geophysical Research: Solid Earth*,
747 112(B1).
- 748 Boneh, Y., Schottenfels, E., Kwong, K., Van Zelst, I., Tong, X., Eimer, M., ...
749 Zhan, Z. (2019). Intermediate-depth earthquakes controlled by incoming plate
750 hydration along bending-related faults. *Geophysical Research Letters*, 46(7),
751 3688–3697. Retrieved from [https://agupubs.onlinelibrary.wiley.com/
752 doi/abs/10.1029/2018GL081585](https://agupubs.onlinelibrary.wiley.com/doi/abs/10.1029/2018GL081585) doi: 10.1029/2018GL081585
- 753 Borrelli, M. E., O'Rourke, J. G., Smrekar, S. E., & Ostberg, C. M. (2021). A Global
754 Survey of Lithospheric Flexure at Steep-Sided Domical Volcanoes on Venus
755 Reveals Intermediate Elastic Thicknesses. *Journal of Geophysical Research:*
756 *Planets*, 126(7), e2020JE006756.
- 757 Brissaud, Q., Krishnamoorthy, S., Jackson, J. M., Bowman, D. C., Komjathy, A.,
758 Cutts, J. A., ... Walsh, G. J. (2021). The first detection of an earthquake
759 from a balloon using its acoustic signature. *Geophysical Research Letters*,
760 48(12), e2021GL093013.
- 761 Brossier, J., Gilmore, M. S., & Head, J. W. (2022). Extended Rift-Associated Vol-
762 canism in Ganis Chasma, Venus Detected From Magellan Radar Emissivity.
763 *Geophysical Research Letters*, 49(15), e2022GL099765.
- 764 Bulmer, M., & Guest, J. (1996). Modified volcanic domes and associated debris
765 aprons on Venus. *Geological Society, London, Special Publications*, 110(1),
766 349–371.
- 767 Bulmer, M., Petley, D., Murphy, W., & Mantovani, F. (2006). Detecting slope de-
768 formation using two-pass differential interferometry: Implications for landslide
769 studies on Earth and other planetary bodies. *Journal of Geophysical Research:*
770 *Planets*, 111(E6).
- 771 Bulmer, M. H. K. (2012). Landslides on other planets. In J. J. Clague & D. Stead
772 (Eds.), *Landslides: Types, mechanisms and modeling* (p. 393–408). Cambridge
773 University Press. doi: 10.1017/CBO9780511740367.033
- 774 Byrne, P. K., Ghail, R. C., Şengör, A. C., James, P. B., Klimczak, C., & Solomon,
775 S. C. (2021). A globally fragmented and mobile lithosphere on Venus. *Proceed-*
776 *ings of the National Academy of Sciences*, 118(26).
- 777 Byrne, P. K., & Krishnamoorthy, S. (2022). Estimates on the frequency of vol-
778 canic eruptions on Venus. *Journal of Geophysical Research: Planets*, 127(1),

- 779 e2021JE007040. doi: 10.1029/2021JE007040
- 780 Chen, W.-P., & Molnar, P. (1983). Focal depths of intracontinental and intraplate
781 earthquakes and their implications for the thermal and mechanical properties
782 of the lithosphere. *Journal of Geophysical Research: Solid Earth*, 88(B5),
783 4183–4214.
- 784 Davaille, A., Smrekar, S. E., & Tomlinson, S. (2017). Experimental and observa-
785 tional evidence for plume-induced subduction on Venus. *Nature Geoscience*,
786 10(5), 349–355.
- 787 David Nichols. (2022; retrieved: February 16, 2023). *Coloring for Colorblindness*.
788 (<http://tsitsul.in/blog/coloropt/>)
- 789 Dombard, A. J., Johnson, C. L., Richards, M. A., & Solomon, S. C. (2007). A mag-
790 matic loading model for coronae on Venus. *Journal of Geophysical Research:*
791 *Planets*, 112(E4).
- 792 Dragonì, M., & Piombo, A. (2003). A model for the formation of wrinkle ridges in
793 volcanic plains on venus. *Physics of the Earth and Planetary Interiors*, 135(2-
794 3), 161–171.
- 795 Dziewonski, A. M., Chou, T.-A., & Woodhouse, J. H. (1981). Determination of
796 earthquake source parameters from waveform data for studies of global and
797 regional seismicity. *Journal of Geophysical Research: Solid Earth*, 86(B4),
798 2825–2852.
- 799 Ekström, G., Nettles, M., & Dziewoński, A. (2012). The global CMT project 2004–
800 2010: Centroid-moment tensors for 13,017 earthquakes. *Physics of the Earth*
801 *and Planetary Interiors*, 200, 1–9.
- 802 Emmerson, B., & McKenzie, D. (2007). Thermal structure and seismicity of sub-
803 ducting lithosphere. *Physics of the Earth and Planetary Interiors*, 163(1-4),
804 191–208.
- 805 Filiberto, J., Trang, D., Treiman, A. H., & Gilmore, M. S. (2020). Present-day
806 volcanism on Venus as evidenced from weathering rates of olivine. *Science Ad-*
807 *vances*, 6(1), eaax7445.
- 808 Foley, B. J., Bercovici, D., & Landuyt, W. (2012). The conditions for plate tecton-
809 ics on super-earths: inferences from convection models with damage. *Earth and*
810 *Planetary Science Letters*, 331, 281–290.
- 811 Foster, A., & Nimmo, F. (1996). Comparisons between the rift systems of East
812 Africa, Earth and Beta Regio, Venus. *Earth and Planetary Science Letters*,
813 143(1-4), 183–195. doi: 10.1016/0012-821X(96)00146-X
- 814 Frank, S. L., & Head, J. W. (1990). Ridge belts on venus: Morphology and origin.
815 *Earth, Moon, and Planets*, 50, 421–470.
- 816 Ganesh, I., Herrick, R. R., & Kremic, T. (2023). Bounds on Venus’s seismicity from
817 theoretical and analog estimations. In *LPSC Abstracts, No. 2806*.
- 818 Garcia, R. F., Klotz, A., Hertzog, A., Martin, R., G erier, S., Kassarian, E., . . .
819 Mimoun, D. (2022). Infrasound from large earthquakes recorded on a net-
820 work of balloons in the stratosphere. *Geophysical Research Letters*, 49(15),
821 e2022GL098844.
- 822 Gerya, T. V. (2014). Plume-induced crustal convection: 3d thermomechanical model
823 and implications for the origin of novae and coronae on venus. *Earth and Plan-*
824 *etary Science Letters*, 391, 183–192.
- 825 Ghail, R., Wilson, C. F., & Widemann, T. (2016). EnVision M5 Venus or-
826 biter proposal: Opportunities and challenges. In *Aas/division for plane-*
827 *tary sciences meeting abstracts# 48* (Vol. 48, pp. 216–08). doi: [https://](https://ui.adsabs.harvard.edu/abs/2016DPS....4821608G)
828 ui.adsabs.harvard.edu/abs/2016DPS....4821608G
- 829 Gillmann, C., Way, M. J., Avice, G., Breuer, D., Golabek, G. J., H oning, D., . . .
830 others (2022). The long-term evolution of the atmosphere of venus: Processes
831 and feedback mechanisms: Interior-exterior exchanges. *Space Science Reviews*,
832 218(7), 56.
- 833 Gilmore, M., Mueller, N., & Helbert, J. (2015). VIRTIS emissivity of Alpha Re-

- 834 gio, Venus, with implications for tessera composition. *Icarus*, *254*, 350–361.
835 Retrieved from <https://doi.org/10.1016/j.icarus.2015.04.008> doi:
836 10.1016/j.icarus.2015.04.008
- 837 Gilmore, M. S., Darby Dyar, M., Mueller, N., Brossier, J., Santos, A. R., Ivanov,
838 M., ... Helbert, J. (2023). Mineralogy of the Venus surface. *Space Science*
839 *Reviews*, *219*(7), 52.
- 840 Graff, J., Ernst, R. E., & Samson, C. (2018). Evidence for triple-junction rifting
841 focussed on local magmatic centres along Parga Chasma, Venus. *Icarus*, *306*,
842 122–138.
- 843 Green, H. W., & Houston, H. (1995). The mechanics of deep earthquakes. *Annual*
844 *Review of Earth and Planetary Sciences*, *23*(1), 169–213.
- 845 Grimm, R., & Hess, P. (1997). The crust of venus. *Venus II: Geology, geophysics, at-*
846 *mosphere, and solar wind environment*, 1205.
- 847 Grimm, R. E. (1994). Recent deformation rates on venus. *Journal of Geophysical*
848 *Research: Planets*, *99*(E11), 23163–23171.
- 849 Grinspoon, D. H. (1993). Implications of the high d/h ratio for the sources of water
850 in venus' atmosphere. *Nature*, *363*(6428), 428–431.
- 851 Gülcher, A. J., Gerya, T. V., Montési, L. G., & Munch, J. (2020). Corona struc-
852 tures driven by plume–lithosphere interactions and evidence for ongoing plume
853 activity on Venus. *Nature Geoscience*, *13*(8), 547–554.
- 854 Gülcher, A. J., Yu, T.-Y., & Gerya, T. V. (2023). Tectono-Magmatic Evolution of
855 Asymmetric Coronae on Venus: Topographic Classification and 3D Thermo-
856 Mechanical Modeling. *Journal of Geophysical Research: Planets*, *128*(11),
857 e2023JE007978.
- 858 Gutenberg, B., & Richter, C. F. (1956). Magnitude and energy of earthquakes. *An-*
859 *nals of Geophysics*, *9*(1), 1–15.
- 860 Gutscher, M.-A., & Peacock, S. M. (2003). Thermal models of flat subduction and
861 the rupture zone of great subduction earthquakes. *Journal of Geophysical Re-*
862 *search: Solid Earth*, *108*(B1), ESE–2.
- 863 Hacker, B. R., Peacock, S. M., Abers, G. A., & Holloway, S. D. (2003). Subduction
864 factory 2. Are intermediate-depth earthquakes in subducting slabs linked to
865 metamorphic dehydration reactions? *Journal of Geophysical Research: Solid*
866 *Earth*, *108*(B1).
- 867 Hahn, R., & Byrne, P. (2023). Characterizing Styles of Volcano Gravitational Deform-
868 ation On Venus. In *Lunar and planetary science conference abstracts 2023*.
- 869 Harris, L. B., & Bédard, J. H. (2015). Interactions between continent-like ‘drift’,
870 rifting and mantle flow on venus: gravity interpretations and earth analogues.
871 *Geological Society, London, Special Publications*, *401*(1), 327–356.
- 872 Hasterok, D., Halpin, J. A., Collins, A. S., Hand, M., Kreemer, C., Gard, M. G., &
873 Glorie, S. (2022). New maps of global geological provinces and tectonic plates.
874 *Earth-Science Reviews*, *231*, 104069.
- 875 He, C., Wang, Z., & Yao, W. (2007). Frictional sliding of gabbro gouge under hy-
876 drothermal conditions. *Tectonophysics*, *445*(3-4), 353–362.
- 877 Head, J. W. (1990). Venus trough-and-ridge tessera: Analog to Earth oceanic crust
878 formed at spreading centers? *Journal of Geophysical Research: Solid Earth*,
879 *95*(B5), 7119–7132.
- 880 Herrick, R. R. (1999). Small mantle upwellings are pervasive on venus and earth.
881 *Geophysical research letters*, *26*(6), 803–806.
- 882 Herrick, R. R., Bjornes, E. T., Carter, L. M., Gerya, T., Ghail, R. C., Gillmann, C.,
883 ... others (2023). Resurfacing history and volcanic activity of venus. *Space*
884 *Science Reviews*, *219*(4), 29.
- 885 Herrick, R. R., & Hensley, S. (2023). Surface changes observed on a Venusian vol-
886 cano during the Magellan mission. *Science*, *379*(6638), 1205–1208. doi: 10
887 .1126/science.abm7735

- 888 Hoogenboom, T., & Houseman, G. A. (2006). Rayleigh–Taylor instability as a mech-
 889 anism for corona formation on Venus. *Icarus*, *180*(2), 292–307.
- 890 Houston, H. (2015). 4.13 - Deep Earthquakes. In G. Schubert (Ed.), *Treatise on geo-*
 891 *physics* (Second ed., p. 329 - 354). Oxford: Elsevier. Retrieved from [http://](http://www.sciencedirect.com/science/article/pii/B9780444538024000798)
 892 www.sciencedirect.com/science/article/pii/B9780444538024000798
 893 doi: <https://doi.org/10.1016/B978-0-444-53802-4.00079-8>
- 894 Hyndman, R. D., & Wang, K. (1993). Thermal constraints on the zone of major
 895 thrust earthquake failure: The cascadia subduction zone. *Journal of Geophysi-*
 896 *cal Research: Solid Earth*, *98*(B2), 2039–2060.
- 897 Hyndman, R. D., Yamano, M., & Oleskevich, D. A. (1997). The seismogenic zone of
 898 subduction thrust faults. *Island Arc*, *6*(3), 244–260.
- 899 Ivanov, M. A., & Head, J. W. (2011). Global geological map of Venus. *Planetary*
 900 *and Space Science*, *59*(13), 1559–1600.
- 901 James, P. B., Zuber, M. T., & Phillips, R. J. (2013). Crustal thickness and support
 902 of topography on Venus. *Journal of Geophysical Research: Planets*, *118*(4),
 903 859–875.
- 904 Janes, D. M., Squyres, S. W., Bindschadler, D. L., Baer, G., Schubert, G., Sharp-
 905 ton, V. L., & Stofan, E. R. (1992). Geophysical models for the formation
 906 and evolution of coronae on Venus. *Journal of Geophysical Research: Planets*,
 907 *97*(E10), 16055–16067.
- 908 Johnson, C. L., & Richards, M. A. (2003). A conceptual model for the relationship
 909 between coronae and large-scale mantle dynamics on venus. *Journal of Geo-*
 910 *physical Research: Planets*, *108*(E6).
- 911 Jull, M. G., & Arkani-Hamed, J. (1995). The implications of basalt in the formation
 912 and evolution of mountains on venus. *Physics of the Earth and Planetary Inte-*
 913 *riors*, *89*(3-4), 163–175.
- 914 Jung, H., Green Ii, H. W., & Dobrzhinetskaya, L. F. (2004). Intermediate-depth
 915 earthquake faulting by dehydration embrittlement with negative volume
 916 change. *Nature*, *428*(6982), 545–549.
- 917 Jurdy, D. M., & Stoddard, P. R. (2007, 01). The coronae of Venus: Impact, plume,
 918 or other origin? In *Plates, Plumes and Planetary Processes*. Geological Society
 919 of America. doi: 10.1130/2007.2430(40)
- 920 Karato, S.-i., & Barbot, S. (2018). Dynamics of fault motion and the origin of con-
 921 trasting tectonic style between Earth and Venus. *Scientific Reports*, *8*(1), 1–
 922 11.
- 923 Kelemen, P. B., & Hirth, G. (2007). A periodic shear-heating mechanism for
 924 intermediate-depth earthquakes in the mantle. *Nature*, *446*(7137), 787–790.
- 925 Kiefer, W. S., & Peterson, K. (2003). Mantle and crustal structure in phoebe
 926 regio and devana chasma, venus. *Geophysical Research Letters*, *30*(1), 5-1-5-
 927 4. Retrieved from [https://agupubs.onlinelibrary.wiley.com/doi/abs/](https://agupubs.onlinelibrary.wiley.com/doi/abs/10.1029/2002GL015762)
 928 [10.1029/2002GL015762](https://agupubs.onlinelibrary.wiley.com/doi/abs/10.1029/2002GL015762)
- 929 Kiefer, W. S., & Swafford, L. C. (2006). Topographic analysis of Devana Chasma,
 930 Venus: Implications for rift system segmentation and propagation. *Journal of*
 931 *structural geology*, *28*(12), 2144–2155.
- 932 Koch, D. M., & Manga, M. (1996). Neutrally buoyant diapirs: A model for venus
 933 coronae. *Geophysical Research Letters*, *23*(3), 225–228.
- 934 Kremic, T., Ghail, R., Gilmore, M., Hunter, G., Kiefer, W., Limaye, S., . . . Wilson,
 935 C. (2020). Long-duration Venus lander for seismic and atmospheric science.
 936 *Planetary and space science*, *190*, 104961. doi: [https://doi.org/10.1016/](https://doi.org/10.1016/j.pss.2020.104961)
 937 [j.pss.2020.104961](https://doi.org/10.1016/j.pss.2020.104961)
- 938 Krishnamoorthy, S., & Bowman, D. C. (2023). A “Floatilla” of Airborne Seismome-
 939 ters for Venus. *Geophysical Research Letters*, *50*(2), e2022GL100978.
- 940 Krishnamoorthy, S., Komjathy, A., Cutts, J. A., Lognonne, P., Garcia, R. F., Pan-
 941 ning, M. P., . . . others (2020). *Seismology on Venus with infrasound obser-*
 942 *vations from balloon and orbit* (Tech. Rep.). Sandia National Lab.(SNL-NM),

- 943 Albuquerque, NM (United States).
- 944 Kryuchkov, V. (1990). Ridge belts: Are they compressional or extensional structures? *Earth, Moon, and Planets*, *50*(1), 471–491.
- 945
- 946 Ksanfomaliti, L., Zubkova, V., Morozov, N., & Petrova, E. (1982). Microseisms at
947 the VENERA-13 and VENERA-14 Landing Sites. *Soviet Astronomy Letters*,
948 *8*, 241.
- 949 Le Feuvre, M., & Wieczorek, M. A. (2011). Nonuniform cratering of the Moon
950 and a revised crater chronology of the inner Solar System. *Icarus*, *214*(1), 1–
951 20. Retrieved from <https://doi.org/10.1016/j.icarus.2011.03.010> doi:
952 10.1016/j.icarus.2011.03.010
- 953 Lenardic, A., Jellinek, A., & Moresi, L.-N. (2008). A climate induced transition in
954 the tectonic style of a terrestrial planet. *Earth and Planetary Science Letters*,
955 *271*(1-4), 34–42.
- 956 Lognonné, P., & Johnson, C. (2015). 10.03—planetary seismology. *Treatise on geo-*
957 *physics*, *2*, 65–120.
- 958 Lorenz, R. D. (2012). Planetary seismology—Expectations for lander and wind noise
959 with application to Venus. *Planetary and Space Science*, *62*(1), 86–96.
- 960 Lourenço, D. L., Rozel, A. B., Ballmer, M. D., & Tackley, P. J. (2020). Plutonic-
961 squishy lid: a new global tectonic regime generated by intrusive magma-
962 tism on Earth-like planets. *Geochemistry, Geophysics, Geosystems*, *21*(4),
963 e2019GC008756.
- 964 Mackwell, S., Zimmerman, M., & Kohlstedt, D. (1998). High-temperature deformation
965 of dry diabase with application to tectonics on venus. *Journal of Geophys-*
966 *ical Research: Solid Earth*, *103*(B1), 975–984.
- 967 Maia, J. S., & Wieczorek, M. A. (2022). Lithospheric Structure of Venusian Crustal
968 Plateaus. *Journal of Geophysical Research: Planets*, e2021JE007004.
- 969 Marcq, E., Bertaux, J.-L., Montmessin, F., & Belyaev, D. (2013). Variations of
970 sulphur dioxide at the cloud top of Venus’s dynamic atmosphere. *Nature geo-*
971 *science*, *6*(1), 25–28. doi: <https://doi.org/10.1038/ngeo1650>
- 972 McGill, G. E., Steenstrup, S. J., Barton, C., & Ford, P. G. (1981). Continental
973 rifting and the origin of beta regio, venus. *Geophysical Research Letters*, *8*(7),
974 737–740.
- 975 McKenzie, D., Jackson, J., & Priestley, K. (2005). Thermal structure of oceanic and
976 continental lithosphere. *Earth and Planetary Science Letters*, *233*(3-4), 337–
977 349.
- 978 McKinnon, W. B., Zahnle, K. J., Ivanov, B. A., & Melosh, H. (1997). Cratering on
979 Venus: Models and observations. *Venus II: Geology, geophysics, atmosphere,*
980 *and solar wind environment*, 969.
- 981 Melgar, D., Ruiz-Angulo, A., Garcia, E. S., Manea, M., Manea, V. C., Xu, X., ...
982 others (2018). Deep embrittlement and complete rupture of the lithosphere
983 during the m w 8.2 tehuantepec earthquake. *Nature Geoscience*, *11*(12),
984 955–960.
- 985 Molnar, P. (2020). The brittle-plastic transition, earthquakes, temperatures,
986 and strain rates. *Journal of Geophysical Research: Solid Earth*, *125*(7),
987 e2019JB019335.
- 988 Musser Jr, G. S., & Squyres, S. W. (1997). A coupled thermal-mechanical model
989 for corona formation on venus. *Journal of Geophysical Research: Planets*,
990 *102*(E3), 6581–6595.
- 991 Nakamura, Y., Latham, G. V., & Dorman, H. J. (1982). Apollo lunar seismic experi-
992 ment—Final summary. *Journal of Geophysical Research: Solid Earth*, *87*(S01),
993 A117–A123.
- 994 Namiki, N., & Solomon, S. C. (1998). Volcanic degassing of argon and helium and
995 the history of crustal production on venus. *Journal of Geophysical Research:*
996 *Planets*, *103*(E2), 3655–3677.
- 997 O’Rourke, J., Wilson, C., Borrelli, M., Byrne, P. K., Dumoulin, C., Ghail, R., ...

- 998 Westall, F. (2023). Venus, the Planet: Introduction to the Evolution of Earth’s
999 Sister Planet. *Space Science Reviews*, 219(10).
- 1000 Pavri, B., Head III, J. W., Klose, K. B., & Wilson, L. (1992). Steep-sided domes on
1001 Venus: Characteristics, geologic setting, and eruption conditions from Magellan
1002 data. *Journal of Geophysical Research: Planets*, 97(E8), 13445–13478.
- 1003 Peacock, S. M. (2001). Are the lower planes of double seismic zones caused by ser-
1004 pentine dehydration in subducting oceanic mantle? *Geology*, 29(4), 299–302.
- 1005 Peacock, S. M., & Hyndman, R. D. (1999). Hydrous minerals in the mantle wedge
1006 and the maximum depth of subduction thrust earthquakes. *Geophysical Re-
1007 search Letters*, 26(16), 2517–2520.
- 1008 Phillips, R., Kaula, W., McGill, G., & Malin, M. (1981). Tectonics and evolution of
1009 venus. *Science*, 212(4497), 879–887.
- 1010 Phillips, R. J., & Malin, M. C. (1984). Tectonics of venus. *Annual Review of Earth
1011 and Planetary Sciences*, 12(1), 411–443.
- 1012 Piskorz, D., Elkins-Tanton, L. T., & Smrekar, S. E. (2014). Coronae formation
1013 on venus via extension and lithospheric instability. *Journal of Geophysical Re-
1014 search: Planets*, 119(12), 2568–2582.
- 1015 Price, M., & Suppe, J. (1995). Constraints on the resurfacing history of Venus from
1016 the hypsometry and distribution of volcanism, tectonism, and impact craters.
1017 *Earth, Moon, and Planets*, 71(1-2), 99–145.
- 1018 Price, M., Watson, G., Suppe, J., & Brankman, C. (1996). Dating volcanism and
1019 rifting on Venus using impact crater densities. *Journal of Geophysical Re-
1020 search: Planets*, 101(E2), 4657–4671.
- 1021 Prieto, G. A., Froment, B., Yu, C., Poli, P., & Abercrombie, R. (2017). Earthquake
1022 rupture below the brittle-ductile transition in continental lithospheric mantle.
1023 *Science Advances*, 3(3), e1602642.
- 1024 Regorda, A., Thieulot, C., Van Zelst, I., Erdős, Z., Maia, J., & Buiter, S. (2023).
1025 Rifting Venus: insights from numerical modeling. *Journal of Geophysical
1026 Research: Planets*, 128(3), e2022JE007588. doi: 10.1029/2022JE007588
- 1027 Richards, F., Hoggard, M., Cowton, L., & White, N. (2018). Reassessing the ther-
1028 mal structure of oceanic lithosphere with revised global inventories of basement
1029 depths and heat flow measurements. *Journal of Geophysical Research: Solid
1030 Earth*, 123(10), 9136–9161.
- 1031 Rolf, T., Weller, M., Gülcher, A., Byrne, P., O’Rourke, J. G., Herrick, R., . . . others
1032 (2022). Dynamics and evolution of Venus’ mantle through time. *Space Science
1033 Reviews*, 218(8), 70.
- 1034 Romeo, I., & Turcotte, D. (2008). Pulsating continents on Venus: An explanation
1035 for crustal plateaus and tessera terrains. *Earth and Planetary Science Letters*,
1036 276(1-2), 85–97. Retrieved from [https://doi.org/10.1016/j.epsl.2008.09](https://doi.org/10.1016/j.epsl.2008.09.009)
1037 .009 doi: 10.1016/j.epsl.2008.09.009
- 1038 Sabbeth, L., Smrekar, S., & Stock, J. (2023a). Estimated seismicity of Venusian
1039 wrinkle ridges based on fault scaling relationships. *Earth and Planetary Sci-
1040 ence Letters*, 619, 118308. Retrieved from [https://www.sciencedirect.com/
1041 science/article/pii/S0012821X23003217](https://www.sciencedirect.com/science/article/pii/S0012821X23003217) doi: 10.1016/j.epsl.2023.118308
- 1042 Sabbeth, L., Smrekar, S. E., & Stock, J. M. (2023b). Using InSight data to calibrate
1043 seismicity from remote observations of surface faulting. *Journal of Geophysical
1044 Research: Planets*, 128(6), e2022JE007686. Retrieved from [https://agupubs
1045 .onlinelibrary.wiley.com/doi/abs/10.1029/2022JE007686](https://agupubs.onlinelibrary.wiley.com/doi/abs/10.1029/2022JE007686) doi: 10.1029/
1046 2022JE007686
- 1047 Salvador, A., Avice, G., Breuer, D., Gillmann, C., Jacobson, S., Lammer, H., . . .
1048 others (2022). Magma ocean, water, and the early atmosphere of venus. *Space
1049 Sci Rev.*
- 1050 Scholz, C. H. (2019). *The mechanics of earthquakes and faulting*. Cambridge univer-
1051 sity press.
- 1052 Schools, J., & Smrekar, S. (2023). High resolution numerical models of corona for-

- 1053 mation integrating magmatic processes, surface fracturing, and eclogitization.
 1054 *LPI Contributions, 2806*, 1771.
- 1055 Schubert, G., & Sandwell, D. (1995). A global survey of possible subduction sites on
 1056 venus. *Icarus, 117*(1), 173–196.
- 1057 Seno, T. (2009). Determination of the pore fluid pressure ratio at seismogenic
 1058 megathrusts in subduction zones: Implications for strength of asperities and
 1059 Andean-type mountain building. *Journal of Geophysical Research: Solid Earth,*
 1060 *114*(B5).
- 1061 Seton, M., Müller, R. D., Zahirovic, S., Williams, S., Wright, N. M., Cannon, J., ...
 1062 McGirr, R. (2020). A global data set of present-day oceanic crustal age and
 1063 seafloor spreading parameters. *Geochemistry, Geophysics, Geosystems, 21*(10),
 1064 e2020GC009214.
- 1065 Smrekar, S. E., Davaille, A., & Sotin, C. (2018). Venus interior structure and dy-
 1066 namics. *Space Science Reviews, 214*(5), 1–34.
- 1067 Smrekar, S. E., Dyar, D., Helbert, J., Hensley, S., Nunes, D., & Whitten, J. (2020).
 1068 VERITAS (Venus Emissivity, Radio Science, InSAR, Topography, and Spec-
 1069 troscopy): A proposed Discovery mission. In *European planetary science*
 1070 *congress* (p. EPSC2020-447). doi: <https://doi.org/10.5194/epsc2020-447>
- 1071 Smrekar, S. E., Ostberg, C., & O'Rourke, J. G. (2023). Earth-like lithospheric thick-
 1072 ness and heat flow on Venus consistent with active rifting. *Nature Geoscience,*
 1073 *16*(1), 13–18.
- 1074 Smrekar, S. E., & Sotin, C. (2012). Constraints on mantle plumes on venus: Implica-
 1075 tions for volatile history. *Icarus, 217*(2), 510–523.
- 1076 Smrekar, S. E., & Stofan, E. R. (1997). Corona formation and heat loss on venus by
 1077 coupled upwelling and delamination. *Science, 277*(5330), 1289–1294.
- 1078 Smrekar, S. E., & Stofan, E. R. (1999). Origin of corona-dominated topographic
 1079 rises on venus. *Icarus, 139*(1), 100–115.
- 1080 Smrekar, S. E., Stofan, E. R., Mueller, N., Treiman, A., Elkins-Tanton, L., Helbert,
 1081 J., ... Drossart, P. (2010). Recent hotspot volcanism on Venus from VIRTIS
 1082 emissivity data. *Science, 328*(5978), 605–608. doi: [https://doi.org/10.1126/](https://doi.org/10.1126/science.1186785)
 1083 [science.1186785](https://doi.org/10.1126/science.1186785)
- 1084 Solomon, S. (1993). The geophysics of venus. *Physics Today, 46*(7), 48–55.
- 1085 Solomon, S. C., Bullock, M. A., & Grinspoon, D. H. (1999). Climate change as a
 1086 regulator of tectonics on venus. *Science, 286*(5437), 87–90.
- 1087 Spencer, J. E. (2001). Possible giant metamorphic core complex at the center of
 1088 artemis corona, venus. *Geological Society of America Bulletin, 113*(3), 333–
 1089 345.
- 1090 Squyres, S. W., Janes, D., Baer, G., Bindschadler, D. L., Schubert, G., Sharpton,
 1091 V. L., & Stofan, E. R. (1992). The morphology and evolution of coronae on
 1092 venus. *Journal of Geophysical Research: Planets, 97*(E8), 13611–13634.
- 1093 Stein, S., & Wysession, M. (2009). *An introduction to seismology, earthquakes, and*
 1094 *earth structure*. John Wiley & Sons.
- 1095 Stevenson, D. J., Cutts, J. A., Mimoun, D., Arrowsmith, S., Banerdt, W. B., Blom,
 1096 P., ... others (2015). Probing the interior structure of Venus.
- 1097 Stoddard, P. R., & Jurdy, D. M. (2012). Topographic comparisons of uplift fea-
 1098 tures on Venus and Earth: Implications for Venus tectonics. *Icarus, 217*(2),
 1099 524–533.
- 1100 Stofan, E., Saunders, R., Senske, D., Nock, K., Tralli, D., Lundgren, P., ... others
 1101 (1993). Venus interior structure mission (vism): Establishing a seismic network
 1102 on venus. In *Advanced technologies for planetary instruments*.
- 1103 Stofan, E. R., Bindschadler, D. L., Head, J. W., & Parmentier, E. M. (1991).
 1104 Corona structures on venus: Models of origin. *Journal of Geophysical Re-*
 1105 *search: Planets, 96*(E4), 20933–20946.
- 1106 Stofan, E. R., Sharpton, V. L., Schubert, G., Baer, G., Bindschadler, D. L., Janes,
 1107 D. M., & Squyres, S. W. (1992). Global distribution and characteristics of

- 1108 coronae and related features on Venus: Implications for origin and relation
 1109 to mantle processes. *Journal of Geophysical Research: Planets (1991–2012)*,
 1110 *97*(E8), 13347–13378.
- 1111 Stofan, E. R., Smrekar, S. E., Bindschadler, D. L., & Senske, D. A. (1995). Large
 1112 topographic rises on Venus: Implications for mantle upwelling. *Journal of Geo-*
 1113 *physical Research: Planets*, *100*(E11), 23317–23328. doi: 10.1029/95JE01834
- 1114 Strom, R. G., Schaber, G. G., & Dawson, D. D. (1994). The global resurfacing of
 1115 Venus. *Journal of Geophysical Research: Planets (1991–2012)*, *99*(E5), 10899–
 1116 10926.
- 1117 Tian, Y., Herrick, R. R., West, M. E., & Kremic, T. (2023). Mitigating Power and
 1118 Memory Constraints on a Venusian Seismometer. *Seismological Society of*
 1119 *America*, *94*(1), 159–171.
- 1120 Tichelaar, B. W., & Ruff, L. J. (1993). Depth of seismic coupling along subduction
 1121 zones. *Journal of Geophysical Research: Solid Earth*, *98*(B2), 2017–2037.
- 1122 van Dinther, Y., Gerya, T. V., Dalguer, L. A., Corbi, F., Funicello, F., & Mai,
 1123 P. M. (2013). The seismic cycle at subduction thrusts: 2. Dynamic implica-
 1124 tions of geodynamic simulations validated with laboratory models. *Journal of*
 1125 *Geophysical Research: Solid Earth*, *118*(4), 1502–1525.
- 1126 van Dinther, Y., Gerya, T. V., Dalguer, L. A., Mai, P. M., Morra, G., & Giardini,
 1127 D. (2013). The seismic cycle at subduction thrusts: Insights from seismo-
 1128 thermo-mechanical models. *Journal of Geophysical Research: Solid Earth*,
 1129 *118*(12), 6183–6202.
- 1130 van Dinther, Y., Mai, P. M., Dalguer, L. A., & Gerya, T. V. (2014). Modeling the
 1131 seismic cycle in subduction zones: The role and spatiotemporal occurrence of
 1132 off-megathrust earthquakes. *Geophysical Research Letters*, *41*(4), 1194–1201.
- 1133 Van Zelst, I. (2022). Comment on “Estimates on the frequency of volcanic erup-
 1134 tions on Venus” by Byrne & Krishnamoorthy (2022). *Journal of Geophysical*
 1135 *Research: Planets*, *127*(12), e2022JE007448. doi: 10.1029/2022JE007448
- 1136 Van Zelst, I., Maia, J., Plesa, A.-C., Ghail, R., & Spühler, M. (2024). *Data & scripts*
 1137 *- Estimates on the possible annual seismicity of Venus [Data set]*. Zenodo. doi:
 1138 10.5281/zenodo.10539251
- 1139 Van Zelst, I., Thieulot, C., & Craig, T. J. (2023). The effect of temperature-
 1140 dependent material properties on simple thermal models of subduction zones.
 1141 *Solid Earth*, *14*(7), 683–707. Retrieved from [https://se.copernicus.org/](https://se.copernicus.org/articles/14/683/2023/)
 1142 [articles/14/683/2023/](https://se.copernicus.org/articles/14/683/2023/) doi: 10.5194/se-14-683-2023
- 1143 Van Zelst, I., Wollherr, S., Gabriel, A.-A., Madden, E. H., & van Dinther, Y. (2019).
 1144 Modeling megathrust earthquakes across scales: one-way coupling from geo-
 1145 dynamics and seismic cycles to dynamic rupture. *Journal of Geophysical*
 1146 *Research: Solid Earth*, *124*(11), 11414–11446. doi: 10.1029/2019JB017539
- 1147 Wang, J., Zhao, D., & Yao, Z. (2017). Seismic anisotropy evidence for dehydration
 1148 embrittlement triggering intermediate-depth earthquakes. *Scientific reports*,
 1149 *7*(1), 1–9.
- 1150 Weller, M., Lenardic, A., & O’Neill, C. (2015). The effects of internal heating and
 1151 large scale climate variations on tectonic bi-stability in terrestrial planets.
 1152 *Earth and Planetary Science Letters*, *420*, 85–94.
- 1153 Widemann, T., Smrekar, S. E., Garvin, J. B., Straume-Lindner, A. G., Ocampo,
 1154 A. C., Schulte, M. D., ... others (2023). Venus evolution through time: key
 1155 science questions, selected mission concepts and future investigations. *Space*
 1156 *Science Reviews*, *219*(7), 56.
- 1157 Wright, T. J., Elliott, J. R., Wang, H., & Ryder, I. (2013). Earthquake cycle defor-
 1158 mation and the Moho: Implications for the rheology of continental lithosphere.
 1159 *Tectonophysics*, *609*, 504–523.
- 1160 Yamasaki, T., & Seno, T. (2003). Double seismic zone and dehydration embrit-
 1161 tlement of the subducting slab. *Journal of Geophysical Research: Solid Earth*,
 1162 *108*(B4).

1163 Zhong, S.-S., Zhao, Y.-Y. S., Lin, H., Chang, R., Qi, C., Wang, J., ... others (2023).
 1164 High-temperature oxidation of magnesium-and iron-rich olivine under a co2
 1165 atmosphere: Implications for venus. *Remote Sensing*, 15(8), 1959.
 1166 Zuber, M. (1990). Ridge belts: Evidence for regional-and local-scale deformation on
 1167 the surface of venus. *Geophysical Research Letters*, 17(9), 1369–1372.

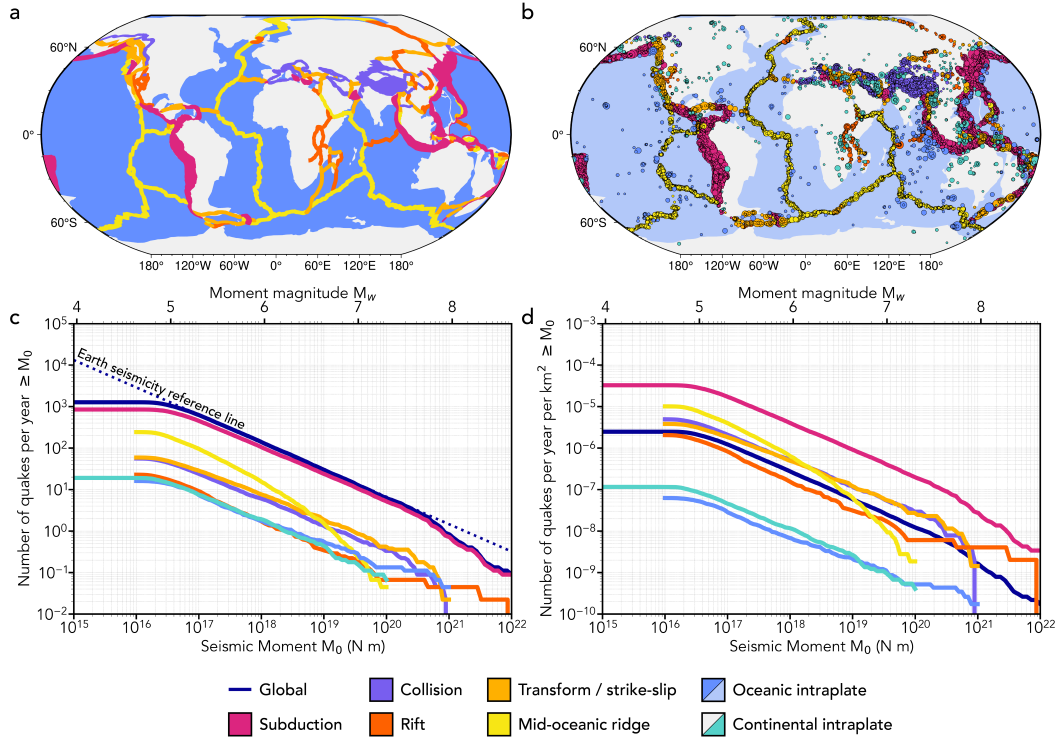


Figure 1. (a) Map of the Earth showing how its surface area is divided into seven discrete tectonic settings. (b) Earthquakes in the CMT catalogue from 1976 - 2020 coloured according to tectonic setting with the symbol size proportional to the earthquake magnitude. (c) Annual earthquake size-frequency distribution for the Earth based on the CMT catalogue and split into different tectonic settings. The dotted dark blue line is a reference line for Earth's seismicity extrapolated from the size-frequency distribution for seismic moments of 10^{17} N m to 10^{19} N m to lower and higher seismic moment assuming a constant slope. Note that this means that the Earth's reference line overestimates the amount of quakes with moment magnitudes larger than 8. (d) Seismicity density on the Earth for different tectonic settings, i.e., number of earthquakes in the CMT catalogue per year per km^2 . Maps are in Robinson projection.

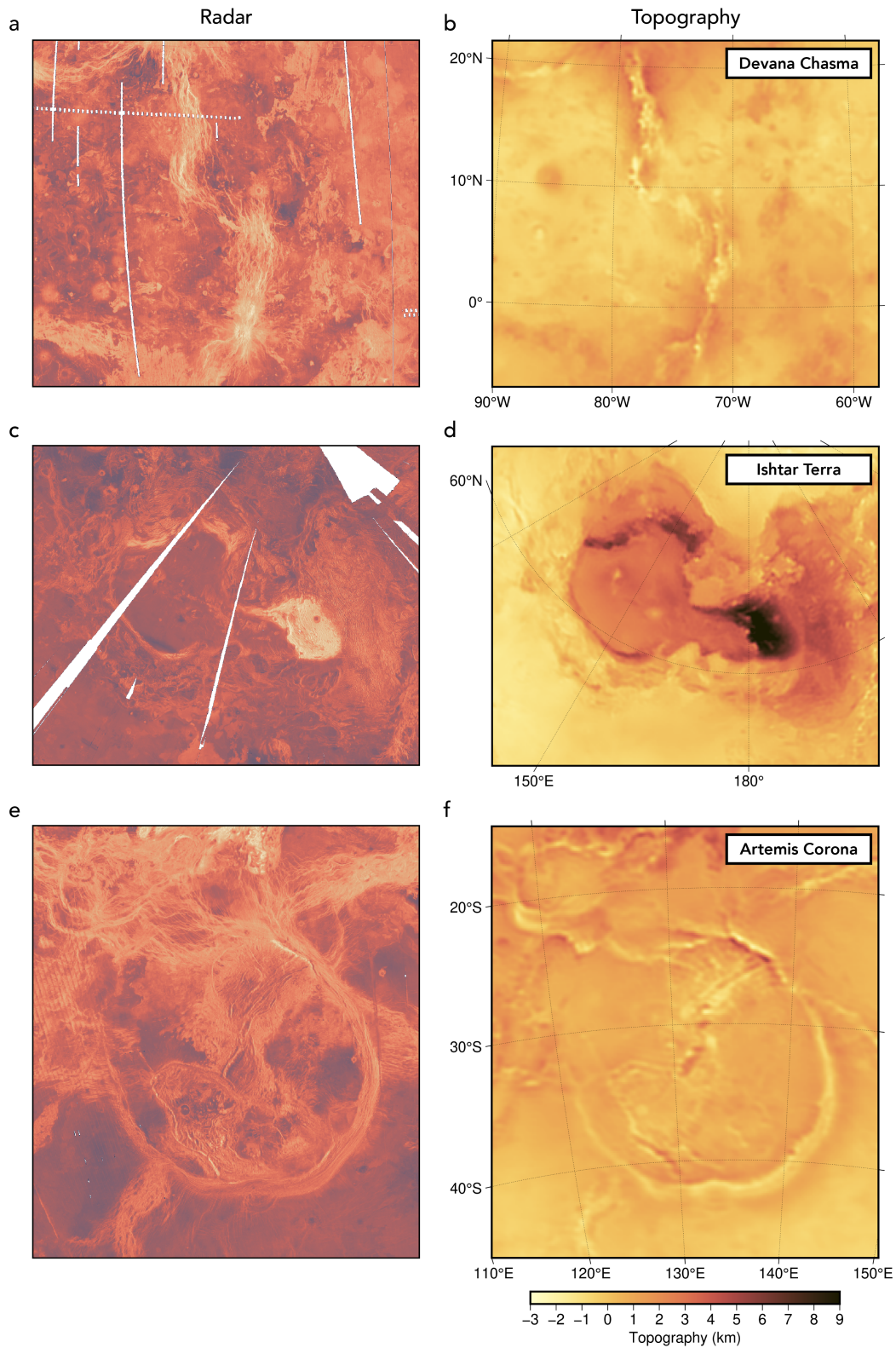


Figure 2. Examples of tectonic features on Venus with radar images on the left and topography data on the right. (a) Devana Chasma as an example of a rift system on Venus; (b) Ishtar Terra with Maxwell Montes as an example of a region characterised by compressional deformation and classified as a fold belt in this study following Price et al. (1996); (c) Artemis Corona, the largest corona on Venus. We adopted the Lambert azimuthal equal-area projection to generate these maps.

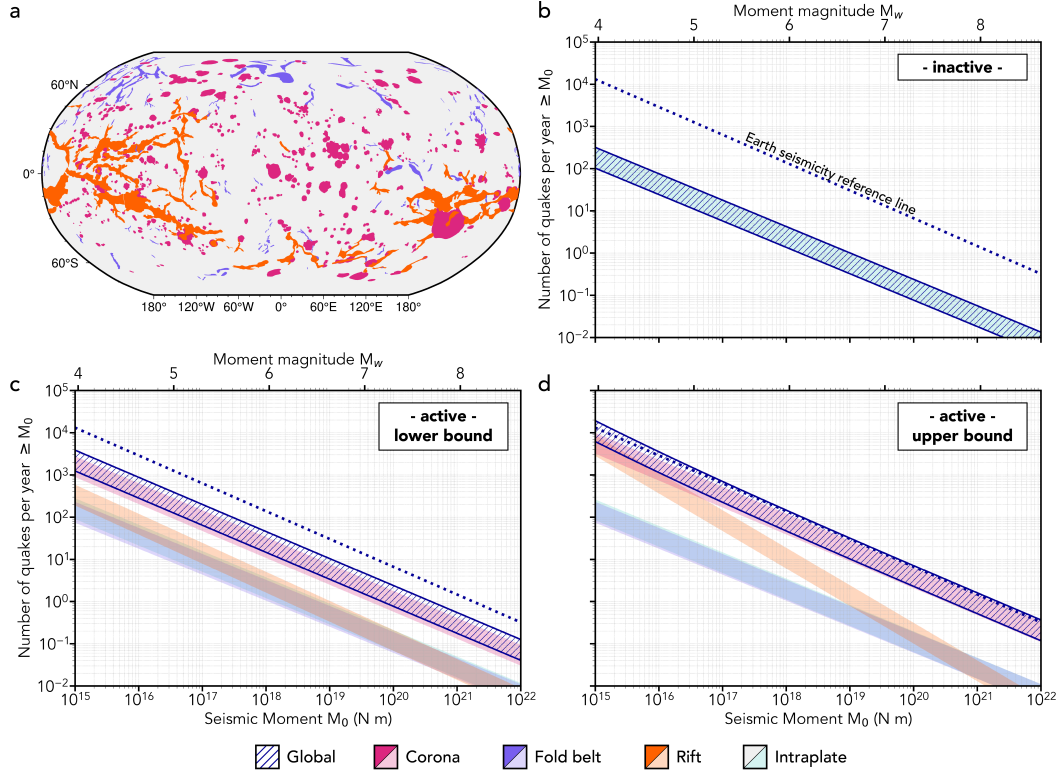


Figure 3. (a) Map of Venus (Robinson projection) showing the areas of mapped coronae, fold belts, and rifts (Price & Suppe, 1995; Price et al., 1996). (b-d) Ranges of potential quake size-frequency distributions on Venus for (b) an inactive Venus with background seismicity analogous to Earth's continental intraplate seismicity; (c) a lower bound on an active Venus; and (d) an upper bound on an active Venus. The hatched area shows the global, accumulated annual seismicity that combines the seismicity of the different individual tectonic settings. Note that because of the log-log scale, the global estimate and the seismicity range of the highest individual tectonic setting are closely-spaced. Dotted dark blue line indicates the reference Earth seismicity line, which corresponds to the slope of the size-frequency distribution for seismic moments of 10^{17} N m to 10^{19} N m of global seismicity on Earth (Figure 1c).